Columnar EEG magnetic influences on molecular development of short-term memory

Lester Ingber

Lester Ingber Research
Ashland Oregon USA
ingber@ingber.com, ingber@alumni.caltech.edu
http://www.ingber.com/

Abstract

For several decades the stated Holy Grail of chemical, biological and biophysical research into neocortical information processing has been to reduce such neocortical phenomena into specific bottom-up molecular and smaller-scale processes. Over the past three decades, with regard to short-term memory (STM) and long-term memory (LTM) phenomena, which themselves are likely components of other phenomena like attention and consciousness, a statistical mechanics of neocortical interactions (SMNI) approach has yielded specific details of STM capacity, duration and stability not present in molecular approaches, but it is clear that most molecular approaches consider it inevitable that their reductionist approaches at molecular and possibly even quantum scales will yet prove to be causal explanations of such phenomena. The SMNI approach is a bottom-up aggregation from synaptic scales to columnar and regional scales of neocortex, and has been merged with larger non-invasive EEG scales with other colleagues -- all at scales much coarser than molecular scales. As with many Crusades for some truths, other truths can be trampled. It is proposed that an SMNI vector potential (SMNI-VP) constructed from magnetic fields induced by neuronal electrical firings, at thresholds of collective minicolumnar activity with laminar specification, can give rise to causal top-down mechanisms that effect molecular excitatory and inhibitory processes in STM and LTM. A specific example might be causal influences on momentum $\mathbf{p}$ of Ca^{2+} ions by the SMNI-VP $\mathbf{A}$, as calculated by the canonical momentum Π, $\Pi = \mathbf{p} - q\mathbf{A}$, where $q = -2e$ for Ca^{2+}, e is the electron coulomb charge, which may be applied either classically or quantum-mechanically. Such a smoking gun for top-down effects awaits forensic in vivo experimental verification, requiring appreciating the necessity and due diligence of including true multiple-scale interactions across orders of magnitude in the complex neocortical environment.

PACS: 05.10.Gg, 87.50.yg, 87.19.-j

Keywords: short-term memory, astrocytes, neocortical dynamics, vector potential

---

Most recent drafts are available as http://www.ingber.com/smni11_stm_scales.pdf

$Id: smni11_stm_scales,v 1.60 2012/06/24 14:50:00 ingber Exp ingber $

1. Introduction and Rational

The phenomenon of short-term memory (STM) has many aspects and observed as well as conjectured mechanisms. The approach here is to take one approach based on a statistical mechanics of neocortical interactions (SMNI) which has been successful in calculating several important features of STM based on columnar structures in neocortex. This is taken as starting point to see how complementary processes at some larger and some smaller scales can be bridged to better understand STM

The next section describes the development of SMNI STM, followed by a section devoted to a summary of the mathematical development of SMNI. This helps to keep the rest of the paper relatively clear of some of these details, while still giving sufficient background to explain the development. The following section describes a larger context of STM, taking into account other work on smaller scales of neuronal as astrocyte interactions, as well as how the SMNI processes at columnar scales effects larger-scale regional activity. This discussion is conveniently described as bottom-up versus top-down processes. The following section deals with how SMNI processes at columnar scales, tuned to STM processing, can affect molecular scales of activity, via the electromagnetic vector potential, thereby describing a process that requires a casual threshold of columnar activity to influence ionic processes strongly implicated in STM at molecular levels. The last section is a conclusion emphasizing the importance of some top-down processes in STM phenomena.

2. SMNI STM

Neocortex has evolved to use minicolumns of neurons interacting via short-ranged interactions in macrocolumns, and interacting via long-ranged interactions across regions of macrocolumns (Mountcastle, 1978; Buxhoeveden & Casanova, 2002; Rakic, 2008). This common architecture processes patterns of information within and among different regions of sensory, motor, associative cortex, etc. The SMNI approach was the first physical application of a nonlinear multivariate calculus developed by other mathematical physicists in the late 1970's to define a statistical mechanics of multivariate nonlinear nonequilibrium systems (Graham, 1977; Langouche *et al*, 1982).

SMNI builds minicolumnar, macrocolumnar, and regional interactions in neocortex. Since 1981, SMNI has been developed to model columns and regions of neocortex, spanning mm to cm of tissue, As depicted in Figure 1, SMNI develops three biophysical scales of neocortical interactions: (a)-(a^*)-(a') microscopic neurons; (b)-(b') mesocolumnar domains; (c)-(c') macroscopic regions. SMNI has developed appropriate conditional probability distributions at each level, aggregating up from the smallest levels of interactions. In (a^*) synaptic inter-neuronal interactions, averaged over by mesocolumns, are phenomenologically described by the mean and variance of a distribution Ψ. Similarly, in (a) intraneuronal transmissions are phenomenologically described by the mean and variance of Γ. Mesocolumnar averaged excitatory (E) and inhibitory (I) neuronal firings M are represented in (a'). In (b) the vertical organization of minicolumns is sketched together with their horizontal stratification, yielding a physiological entity, the mesocolumn. In (b') the overlap of interacting mesocolumns at locations r and r' from times t and $t+\tau$, τ on the order of 10 msec, is sketched. In (c) macroscopic regions of neocortex are depicted as arising from many mesocolumnar domains. (c') sketches how regions may be coupled by long−ranged interactions.

Most of these papers have dealt explicitly with calculating properties of STM and scalp EEG in order to test the basic formulation of this approach (Ingber, 1981; Ingber, 1982; Ingber, 1983; Ingber, 1984; Ingber, 1985b; Ingber, 1985c; Ingber, 1986; Ingber & Nunez, 1990; Ingber, 1991; Ingber, 1992; Ingber, 1994; Ingber & Nunez, 1995; Ingber, 1995a; Ingber, 1995b; Ingber, 1996b; Ingber, 1996a; Ingber, 1997; Ingber, 1998). The SMNI modeling of local mesocolumnar interactions (convergence and divergence between minicolumnar and macrocolumnar interactions) was tested on STM phenomena. The SMNI modeling of macrocolumnar interactions across regions was tested on EEG phenomena.

2.1. STM Capacity

SMNI studies have detailed that maximal numbers of attractors lie within the physical firing space of M^G, where G = {Excitatory, Inhibitory} minicolumnar firings, consistent with experimentally observed capacities of auditory STM (Miller, 1956; Ericsson & Chase, 1982) and visual STM (G. Zhang & Simon,

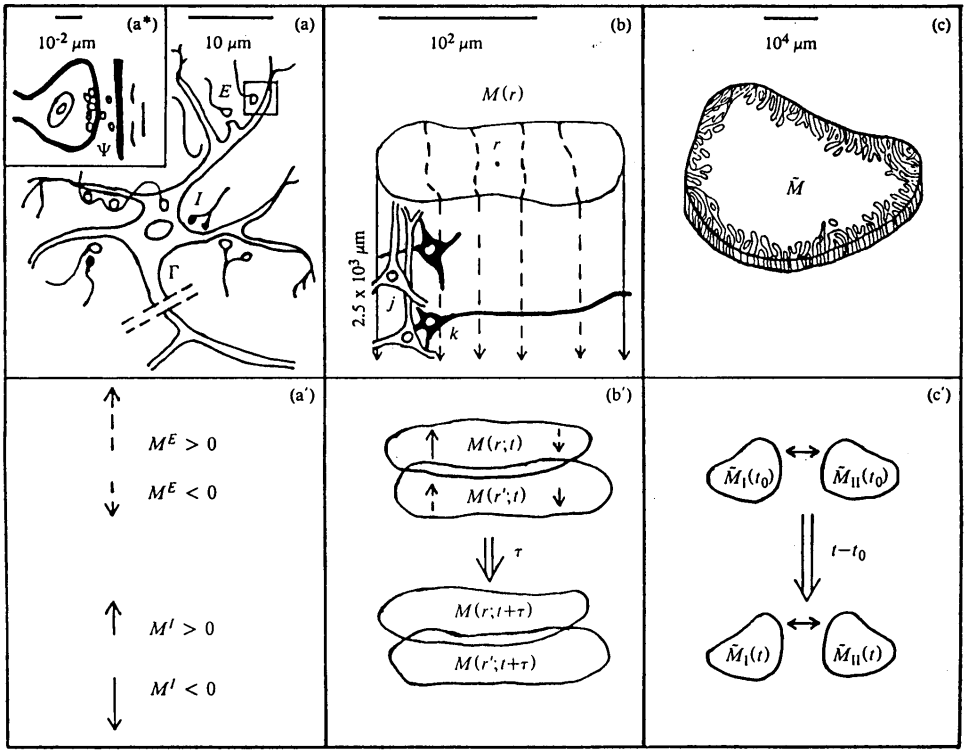

Fig. 1. Illustrated are three biophysical scales of neocortical interactions: (a)-(a*)-(a') microscopic neurons; (b)-(b') mesocolumnar domains; (c)-(c') macroscopic regions. Reprinted with permission from (Ingber, 1983) by the American Physical Society.

1985), when a "centering" mechanism (CM), as detailed below, is enforced by shifting background noise in synaptic interactions, consistent with experimental observations under conditions of selective attention (Mountcastle *et al*, 1981; Ingber, 1984; Ingber, 1985c; Ingber, 1994; Ingber & Nunez, 1995). This leads to all attractors of the short-time distribution lying along a diagonal line in M^G space, effectively defining a narrow parabolic trough containing these most likely firing states. This essentially collapses the two-dimensional M^G space down to a one-dimensional space of most importance. Thus, the predominant physics of STM and of (short-fiber contribution to) EEG phenomena takes place in a narrow "parabolic trough" in M^G space, roughly along a diagonal line (Ingber, 1984).

These calculations were further supported by high-resolution evolution of the two-variable short-time conditional-probability propagator using PATHINT (Ingber & Nunez, 1995). SMNI correctly calculated the stability and duration of STM, random access to memories within tenths of a second as observed, and the observed 7 ± 2 capacity rule of auditory memory (Miller, 1956) and the observed 4 ± 2 capacity rule of visual memory (G. Zhang & Simon, 1985).

Figure 2 shows the evolution of a Balanced Centered model (BC) after 500 foldings of $\Delta t = 0.01$, or 5 unit of relaxation time τ. Note the existence of ten well developed peaks or possible trappings of firing patterns (Ingber & Nunez, 1995). This seems to be able to describe the "7 ± 2" rule. The BC model is described in more detail below.

Figure 3 shows the evolution of a Balanced Centered Visual model (BCV) after 1000 foldings of $\Delta t = 0.01$, or 10 unit of relaxation time τ. Note the existence of four well developed peaks or possible trappings of firing patterns. Also note that other peaks at lower scales are clearly present, numbering on the same order as in the BC' model, as the strength in the original peaks dissipates throughout firing space, but these are much smaller and therefore much less probable to be accessed (Ingber & Nunez, 1995). This seems to be able to describe the "4 ± 2" rule for visual STM.

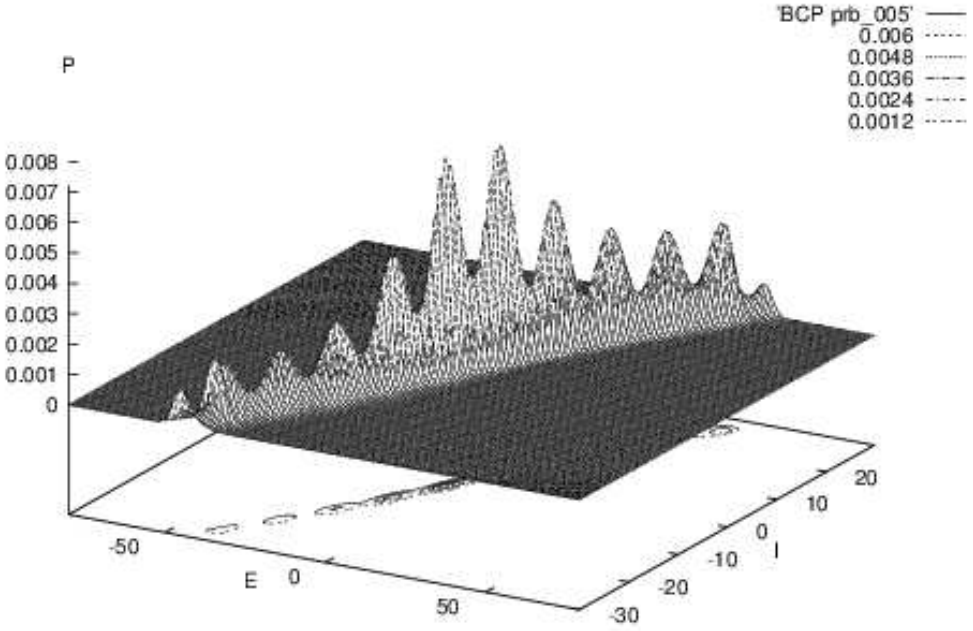

Fig. 2. Illustrated is SMNI STM Model BC at the evolution at 5τ. Reprinted with permission from (Ingber & Nunez, 1995) by the American Physical Society.

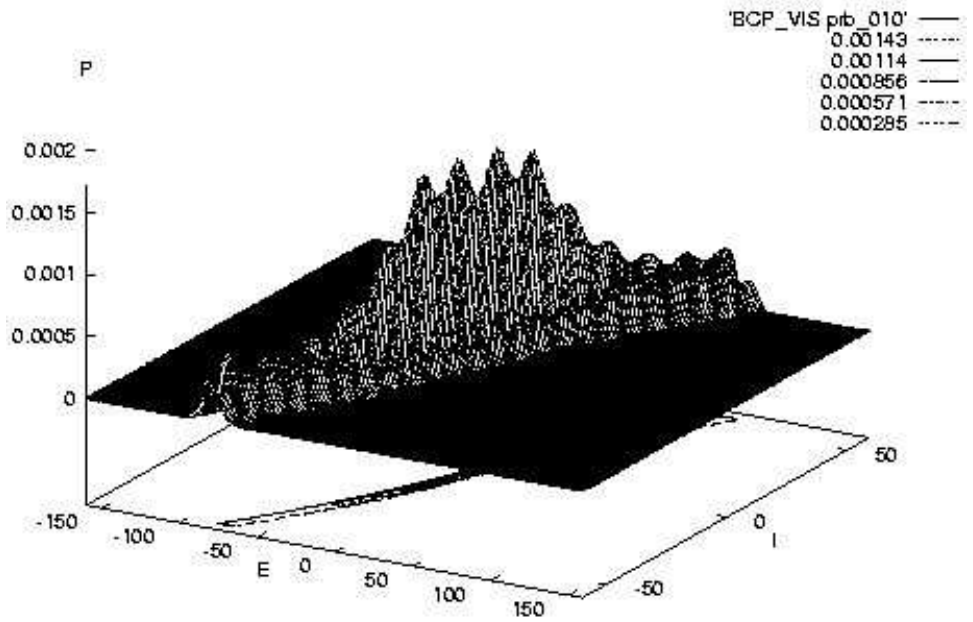

Fig. 3. Illustrated is SMNI STM Model BCV at the evolution at 10τ. Reprinted with permission from (Ingber & Nunez, 1995) by the American Physical Society.

2.2. STM Duration

While early papers (Ingber, 1984; Ingber, 1985c), suggested the possibility of sustenance of STM over epochs of tens of seconds just due to localized columnar interactions, it was clear that longer-ranged influences also are important to the development of the SMNI approach (Ingber, 1981; Ingber, 1982; Ingber, 1983). For example, calculations show that this duration of STM may not be possible if only localized columnar interactions are considered (Ingber, 1994; Ingber & Nunez, 1995). After approximately 5τ, the clear separations between peaks of most-likely states in the evolving conditional probability distribution soon overlap. After approximately 10τ, the separations hardly exists. All four models considered, described below, representing dominant inhibition, dominant excitation, a "balanced"

case in between these two (model BC' illustrated here), and the latter for the visual neocortex, exhibit similar decays of their peaks over these time scales. Future calculations, including all nonlinear SMNI effects might change this numerical result, but still the action of long-ranged neuron-neuron and diffuse neuromodulator interactions are known to be important to neocortical function, and they must be addressed.

2.3. Propagation of Information Across Minicolumns

In the sub-section below on Mathematical Development, it is noted that Euler-Lagrange (EL) equations are derived from the SMNI Lagrangian, the negative of the argument of the exponential describing the short-time conditional probability distribution of columnar firing states. Linearization of the EL equations permits the development of stability analyses and dispersion relations in frequency-wave-number space (Ingber, 1982; Ingber, 1983; Ingber, 1985b). It is noted in this regard that the corresponding wave propagation velocities pace interactions over several minicolumns, of magnitude sufficient to permit simultaneous information processing within about 10^{-1} sec with interactions mediated by long-ranged fibers possessing much greater propagation velocities about 600−900 cm/sec (Ingber, 1985b). E.g., detailed auditory and visual processing can feed information to the association cortex where it can be processed simultaneously, possibly giving feedback to the primary sensory regions. The propagation velocities calculated by SMNI, about 1 cm/sec, also are consistent with observed movements of attention (Tsal, 1983) and of hallucinations (Cowan, 1982) across the visual field. This strongly suggests that nearest-neighbor (NN) mesocolumnar interactions are an important mechanism in these movements.

2.4. Primacy Versus Recency Rule

Another phenomenon of STM capacity explained by the SMNI is the primacy versus recency effect in STM serial processing, wherein first-learned items are recalled most error-free, with last-learned items still more error-free than those in the middle (Murdock, 1983). The primacy versus recency rule is verified for acoustical STM, but visual or semantic STM typically requires longer times for rehearsal in a hypothesized articulatory loop of individual items (G. Zhang & Simon, 1985). In the SMNI approach, the basic assumption is made that a pattern of neuronal firing that persists for many τ cycles is a candidate to store the "memory" of activity that gave rise to this pattern. If several firing patterns can simultaneously exist, then there is the capability of storing several memories. The short-time conditional probability distribution derived for the neocortex is the primary tool to seek such firing patterns. The deepest minima of the Lagrangian, defined below, essentially the argument of this probability distribution, are more likely accessed than the others of this probability distribution, and these valleys are sharper than the others. I.e., they are more readily accessed and sustain their patterns against fluctuations more accurately than the relatively more shallow minima. The more recent memories or newer patterns may be presumed to be those having synaptic parameters more recently tuned and/or more actively rehearsed.

2.5. Hick's Law

SMNI supports random access to memories within tenths of a second as observed, and thereby helps to explain Hick's law of linearity of reaction time (RT) with STM information (Hick, 1952; Jensen, 1987; Ingber, 1999).

The RT necessary to "visit" the states under control during the span of STM can be calculated as the mean time of "first passage" between multiple states of this distribution, in terms of the probability P as an outer integral $\int dt$ (sum) over refraction times of synaptic interactions during STM time t, and an inner integral $\int dM$ (sum) taken over the mesocolumnar firing states M (Risken, 1989), which has been explicitly calculated to be within observed STM time scales (Ingber, 1984),

$$RT = -\int dt \quad t \int dM \, \frac{dP}{dt} \, . \tag{1}$$

The probability distribution P is defined below.

As demonstrated by previous SMNI STM calculations, within tenths of a second, the conditional probability of visiting one state from another P, can be well approximated by a short-time probability distribution expressed in terms of the previously mentioned Lagrangian L as

$$P = \frac{1}{\sqrt{(2\pi dtg)}} \exp(-Ldt) \,, \tag{2}$$

where g is the determinant of the covariance matrix of the distribution P in the space of columnar firings.

This expression for RT can be approximately rewritten as

$$RT \approx K \int dt \int dM \; P \ln P \,, \tag{3}$$

where K is a constant when the Lagrangian is approximately constant over the time scales observed. Since the peaks of the most likely M states of P are to a very good approximation well-separated Gaussian peaks (Ingber, 1984), these states may be treated as independent entities under the integral. This last expression is essentially the "information" content weighted by the time during which processing of information is observed.

The calculation of the heights of peaks corresponding to most likely states includes the combinatoric factors of their possible columnar manifestations as well as the dynamics of synaptic and columnar interactions. In the approximation that we only consider the combinatorics of items of STM as contributing to most likely states measured by P, i.e., that P measures the frequency of occurrences of all possible combinations of these items, we obtain Hick's Law, the observed linear relationship of RT versus STM information storage. For example, when the bits of information are measured by the probability P being the frequency of accessing a given number of items in STM, the bits of information in 2, 4 and 8 states are given as approximately multiples of $\ln 2$ of items, i.e., $\ln 2$, $2 \ln 2$ and $3 \ln 2$, resp. (The limit of taking the logarithm of all combinations of independent items yields a constant times the sum over $p_i \ln p_i$, where p_i is the frequency of occurrence of item i.)

2.6. STM Transference to LTM

SMNI also calculates how STM patterns (e.g., from a given region or even aggregated from multiple regions) may be encoded by dynamic modification of synaptic parameters (within experimentally observed ranges) into long-term memory patterns (LTM) (Ingber, 1983). This calculation simply shows how rates of firing can be encoded into synaptic parameters. It does not address any molecular mechanisms to cause such encodings, e.g., such as those referenced below.

2.7. SMNI Description of EEG

Using the power of the SMNI structure and the optimization algorithm Adaptive Simulated Annealing (ASA), sets of EEG and evoked potential data from an NIH study investigating genetic predispositions to alcoholism (X.L. Zhang *et al*, 1995), were fitted to an SMNI model on a lattice of regional electrodes to extract brain "signatures" of STM (Ingber, 1997; Ingber, 1998). Each electrode site was represented by an SMNI distribution of independent stochastic macrocolumnar-scaled M^G variables, interconnected by long-ranged circuitry with delays appropriate to long-fiber communication in neocortex. The global optimization algorithm ASA was used to perform maximum likelihood fits of Lagrangians defined by path integrals of multivariate conditional probabilities. Canonical momenta indicators (CMI) were thereby derived for individual's EEG data. The CMI give better signal recognition than the raw data, and were used to advantage as correlates of behavioral states. In-sample data was used for training (Ingber, 1997), and out-of-sample data was used for testing (Ingber, 1998) these fits.

These results gave strong quantitative support for an accurate intuitive picture, portraying neocortical interactions as having common algebraic physics mechanisms that scale across quite disparate spatial scales and functional or behavioral phenomena, i.e., describing interactions among neurons, columns of neurons, and regional masses of neurons.

Note that there are other models of EEG which also have sound experimental support. Some of the models can be shown to be indeed complementary to SMNI (Ingber & Nunez, 2010). Scalp potentials (EEG) are generated by synaptic current sources at small scales; each cubic millimeter of cortical tissue

contains more than 100 million synapses. In contrast to this small scale activity, EEG data are recorded at macroscopic (centimeter) scales. All dependent variables are expressed as functions of time and cortical location. The basic approach ignores embedded network activity, although networks have been included in more advanced models (Nunez, 1989; Jirsa & Haken, 1996).

Below, some details of the SMNI approach lead to further confirmation of overlaps with some other approaches to EEG studies.

3. Mathematical Development

3.1. Neuronal Firings from Synaptic Aggregation

Figure 1 gives a visual representation of several stages of aggregation developed in SMNI (Ingber, 1982; Ingber, 1983). Neocortical neurons typically have many dendrites that receive quanta of chemical postsynaptic stimulation from many other neurons. The distribution of quanta transmitted across synapses takes place on the scale of 10^{-2} μm. Each quantum has thousands of molecules of chemical neurotransmitters that affect the chemically gated postsynaptic membrane. Chemical transmissions in the neocortex are believed to be either excitatory (E), such as glutamic acid, or inhibitory (I), such as γ aminobutyric acid. There exist many transmitters as well as other chemicals that modulate their effects, but it is assumed that after millions of synapses between hundreds of neurons are averaged over, then it is reasonable to ascribe a distribution function Ψ with a mean and variance for E and I interneuronal interactions.

Some neuroscientists do not accept the assumption that simple algebraic summation of excitatory depolarizations and inhibitory hyperpolarizations at the base of the inner axonal membrane determines the firing depolarization response of a neuron within its absolute and relative refractory periods (Shepherd, 1979), i.e., including the absolute refractory time after a firing during which no new spikes can be generated, and the relative refractory period during which spikes can be produced only at a decreased sensitivity (Sommerhoff, 1974). However, many other neuroscientists agree that this assumption is reasonable when describing the activity of large ensembles of neocortical neurons, each one typically having many thousands of synaptic interactions.

This same averaging procedure makes it reasonable to ascribe a distribution function Γ with a mean and variance for E and I intraneuronal interactions. A Gaussian Γ is taken to describe the distribution of electrical polarizations caused by chemical quanta impinging on the postsynaptic membrane. These polarizations give a resultant polarization at the base of the neuron, the axon. The base of the axon of a large fiber may be myelinated. However, smaller neurons typically lack these distinguishing features. Experimental techniques are not yet sufficiently advanced to attempt the explicit averaging procedure necessary to establish the means and variances of Ψ and Γ, and their parameters, *in vivo* (Vu & Krasne, 1992). Differential attenuations of polarizations from synapses to the base of an axon are here only phenomenologically accounted for by including these geometric and physiological effects into Γ.

With a sufficient depolarization of approximately 10 to 20 mV at the soma, within an absolute and relative refractory period of approximately 5 msec, an action potential is pulsed down the axon and its many collaterals, affecting voltage-gated presynaptic membranes to release quanta of neurotransmitters. Not detailed here is the biophysics of membranes, of thickness $\approx 5 \times 10^{-3}$ μm, composed of biomolecular leaflets of phospholipid molecules (Caillé *et al*, 1980; Scott, 1975; von der Heydt *et al*, 1981). Ψ and Γ are taken to approximate this biophysics for use in macroscopic studies. Chemical independence of excitatory depolarizations and inhibitory hyperpolarizations are well established in the neocortex, and this independence is retained throughout SMNI.

It should be noted that experimental studies initially used to infer Ψ and Γ (e.g., at neuromuscular junctions) were made possible by deliberately reducing the number of quanta by lowering external calcium concentrations (Boyd & Martin, 1956; Katz, 1966). Ψ was found to be Poissonian, but in that system, where hundreds of quanta are transmitted *in vivo*, Ψ may well be otherwise; for example, Gaussian with independent mean and variance. Current research suggests a binomial distribution, having a Poisson limit (Ingber, 1982; Korn, Mallet & Faber, 1981; Perkel & Feldman, 1979). Note that some investigators have shown a Bernoulli distribution to be more accurate in some cases (Perkel & Feldman,

1979; Ingber, 1982; Korn & Mallet, 1984), and that the very concept of quantal transmission, albeit that good fits to experimental data are achieved with this concept, is under review. In the neocortex, probably small numbers of quanta are transmitted at synapses, but other effects, such as nonuniformity and nonstationarity of presynaptic release sites, and nonlinear summation of postsynaptic potentials, may detract from a simple phenomenological Poisson description (Shepherd, 1979).

This short description serves to point out possible differences in Ψ resulting from many sources. However, the derivation of synaptic interactions given here makes it plausible that for reasonable neuronal parameters, the statistical folding of Ψ and Γ is essentially independent of the functional form assumed for Ψ, just requiring specification of its numerical mean and variance.

The result of this analysis is to calculate the transition probability of the firing of neuron j, p_{σ_j}, given its interaction with its neighbors that also may fire or not fire. The result is given as the tabulated error function. Within the range where the total influences of excitatory and inhibitory firings match and exceed the average threshold potential of a given neuron, the probability of that neuron firing receives its major contribution to increase from 0 towards 1.

This is similar to mathematical results obtained by others (Little, 1974; Little & Shaw, 1978; Shaw & Vasudevan, 1974) who have modeled the neocortex after magnetic systems (Cragg & Temperley, 1954). However, in SMNI, this is derived more generally, and has the neural parameters more specifically denoted with different statistical significances given to Ψ and Γ, as described above.

Consider $10^2 < N < 10^3$ neurons, labeled by k, interacting with a given neuron j. Each neuron may contribute many synaptic interactions to many other neurons. A neuron may have as many as $10^4 - 10^5$ synaptic interactions. Within time $\tau_n \approx 5$ msec, Ψ is the distribution of q quanta of chemical transmitter released from neuron k to neuron j ($k \neq j$) with mean a_{jk}, where

$$a_{jk} = A_{jk}(\sigma_k + 1)/2 + B_{jk} \ . \tag{4}$$

A_{jk} is the conductivity weighting transmission of polarization, dependent on k firing,

$$\sigma_k = \begin{cases} +1, \ k \text{ fires}, \\ -1, \ k \text{ does not fire} \end{cases} \tag{5}$$

and B_{jk} is a background including some nonsynaptic and long-range activity. Of course, A and B are highly complicated functions of kj. This definition of σ_k permits a decomposition of a_{jk} into two different physical contributions.

Further SMNI development yields the conditional probability, p_{σ_j}, of neuron j firing given previous firings within τ of other neurons k:

$$p_{\sigma_j} = \pi^{-\frac{1}{2}} \int_{(\sigma_j F_j \sqrt{\pi}/2)}^{\infty} dz \, \exp(-z^2) \, \tfrac{1}{2} \, [1 - \mathrm{erf}(\sigma_j F_j \sqrt{\pi}/2)],$$

$$F_j = \frac{V_j - \sum_k a_{jk} v_{jk}}{((\pi/2) \sum_{k'} a_{jk'} (v_{jk'}^2 + \phi_{jk'}^2))^{\frac{1}{2}}} \ . \tag{6}$$

"erf" is the tabulated error function, simply related to the normal probability function (Mathews & Walker, 1970). F_j is a "threshold factor," as p_{σ_j} increases from 0 to 1 between $\infty > \sigma_j F_j > -\infty$ sharply within the range of $F_j \approx 0$.

If

$$|\sigma_j F_j| < 1, \tag{7}$$

then an asymptotic expression for p_{σ_j} is

$$p_{\sigma_j} \approx \frac{\exp(-\sigma_j F_j)}{\exp(F_j) + \exp(-F_j)} \ . \tag{8}$$

3.2. Mesocolumns

The SMNI formulation of a multivariate nonlinear nonequilibrium system requires derivation in a proper Riemannian geometry to study proper limits of short-time conditional probability distributions. Prior to the late 1970's and early 1980's, many uses of path integrals for multivariate systems nonlinear in their drifts and diffusions were too cavalier in taking continuum limits. In general, results of derivations may be formally written as continuum limits, but these should be understood to be implemented as discrete in derivations as well as in numerical work (Langouche *et al*, 1982; Schulman, 1981).

A sampling of these details can be seen in the context of SMNI. To properly deal with multivariate nonlinear multiplicative-noise systems, researchers have had to properly discretize the Feynman Lagrangian, L_F, in terms of the Feynman Action $\tilde{S}_F$, including Riemannian induced with the Stratonovich midpoint discretization (Langouche *et al*, 1982). The Einstein convention of summing over factors with repeated indices is assumed. The Feynman probability distribution over the entire cortex, consisting of Λ mesocolumns spanning a total cortical area Ω, can be written formally, i.e., with discretization understood to be necessary in all derived uses and numerical calculations, as

$$\tilde{S}_F = \min \Lambda\Omega^{-1} \int dt' \int d^2r \, L_F \ ,$$

$$L_F = \frac{1}{2} N^{-1}(\dot{M}^G - h^G) g_{GG'}(M^{G'} - h^{G'}) - V \ ,$$

$$h^G = g^G - \frac{1}{2} g^{-1/2}(g^{1/2} g^{GG'})_{,G'} \ ,$$

$$V = V' - (\frac{1}{2} h^G_{;G} + R/6)/N \ ,$$

$$V' = V'^E + V'^I - M^G J_G/(2N\tau) \ ,$$

$$h^G_{;G} = g^{-1/2}(g^{1/2} h^G)_{,G} \ ,$$

$$g = ||g_{GG'}|| = \det(g_{GG'}) = g_{EE} g_{II} \ ,$$

$$g_{GG'} = (g^{GG'})^{-1} \ ,$$

$$R = g^{-1}(g_{EE,II} + g_{II,EE}) - \frac{1}{2} g^{-2} \times \{g_{II}[g_{EE,E} g_{II,E} + (g_{EE,I})^2] + g_{EE}[g_{II,I} g_{EE,I} + (g_{II,E})^2]\} \ ,$$

$$[\cdots]_{,G} \equiv (\partial/\partial M^G)[\cdots] \ . \qquad (9)$$

The Riemannian curvature R arises from the nonlinear inverse variance $g_{GG'}$, which is a *bona fide* metric of this parameter space (Graham, 1978). The discretization of the determinant prefactor of the conditional probability distribution requires additional care (Langouche *et al*, 1982).

Some of the algebra behind SMNI depicts variables and distributions that populate each representative macrocolumn in each region. While Riemannian terms were calculated when using the Stratonovich midpoint discretization of the probability distribution (Ingber, 1982; Ingber, 1983), in order to explicitly deal with the multivariate nonlinearities, here it suffices to use the more readable Ito prepoint discretization, which is an equivalent numerical distribution when used consistently (Langouche *et al*, 1982). Codes for all SMNI algebra were written in several languages and found to give the same numerical answers: algebraic languages Macsyma (and its later version Maxima) and Reduce, Fortran and C, and alphanumeric coding of magnetic strips for the hand calculator HP-41C.

A derived mesoscopic Lagrangian L_M defines the short-time probability distribution of firings in a minicolumn, composed of about 10^2 neurons, given its just previous interactions with all other neurons in its macrocolumnar surround. G is used to represent excitatory (E) and inhibitory (I) contributions. $\bar{G}$ designates contributions from both E and I.

$$P_M = \prod_G P_M^G[M^G(r;t+\tau)|M^{\bar{G}}(r';t)]$$

$$= \sum_{\sigma_j} \delta\left(\sum_{jE}\sigma_j - M^E(r;t+\tau)\right)\delta\left(\sum_{jI}\sigma_j - M^I(r;t+\tau)\right)\prod_j^N p_{\sigma_j}$$

$$\approx \prod_G (2\pi\tau g^{GG})^{-1/2}\exp(-N\tau L_M^G) ,$$

$$P_M \approx (2\pi\tau)^{-1/2} g^{1/2}\exp(-N\tau L_M) ,$$

$$L_M = L_M^E + L_M^I = (2N)^{-1}(\dot{M}^G - g^G)g_{GG'}(\dot{M}^{G'} - g^{G'}) + M^G J_G/(2N\tau) - V' ,$$

$$V' = \sum_G V''^G_{G'}(\rho\nabla M^{G'})^2 ,$$

$$g^G = -\tau^{-1}(M^G + N^G\tanh F^G) ,\ g^{GG'} = (g_{GG'})^{-1} = \delta_G^{G'}\tau^{-1}N^G\mathrm{sech}^2 F^G \ ,\ g = \det(g_{GG'}) ,$$

$$F^G = \frac{(V^G - a_{G'}^{|G|}v_{G'}^{|G|}N^{G'} - \frac{1}{2}A_{G'}^{|G|}v_{G'}^{|G|}M^{G'})}{\left((\pi/2)[(v_{G'}^{|G|})^2 + (\phi_{G'}^{|G|})^2](a_{G'}^{|G|}N^{G'} + \frac{1}{2}A_{G'}^{|G|}M^{G'})\right)^{1/2}} , a_{G'}^G = \frac{1}{2}A_{G'}^G + B_{G'}^G , \quad (10)$$

where $A_{G'}^G$ and $B_{G'}^G$ are minicolumnar-averaged inter-neuronal synaptic efficacies, $v_{G'}^G$ and $\phi_{G'}^G$ are averaged means and variances of contributions to neuronal electric polarizations. $M^{G'}$ and $N^{G'}$ in F^G are afferent macrocolumnar firings, scaled to efferent minicolumnar firings by $N/N* \approx 10^{-3}$, where $N*$ is the number of neurons in a macrocolumn, about 10^5. Similarly, $A_G^{G'}$ and $B_G^{G'}$ have been scaled by $N*/N \approx 10^3$ to keep F^G invariant. V' is mesocolumnar NN interactions. Other values taken are consistent with experimental data, e.g., $V^G = 10$ mV, $v_{G'}^G = 0.1$ mV, $\phi_{G'}^G = 0.03^{1/2}$ mV. Note that these values and the factor $(\pi/2)^{1/2}$ in the denominator of F^G, give identical numerical values for F^G as in earlier papers with values of $\phi_{G'}^G = 0.1$ mV and a factor $\pi^{1/2}$.

It is notes that, as originally derived (Ingber, 1982; Ingber, 1983), the numerator of F^G contains information derived from presynaptic firing interactions. The location of most stable states of this SMNI system is highly dependent on the interactions presented in this numerator. The denominator of F^G contains information derived from factors of presynaptic and postsynaptic neuromodular and electrical processing of these firings. The nonlinearities present in this denominator dramatically affect the number and nature of stable states at scales zoomed in at magnifications on the order of a thousand times, representing neocortical processing of detailed information within a sea of stochastic activity.

3.3. Inclusion of Macroscopic Circuitry

The most important features of this development are described by the Lagrangian L^G and the "threshold factor" F^G describing an important sensitivity of the distribution to changes in its variables and parameters.

To more properly include long-ranged fibers between macrocolumns, the J_G terms can be dropped, and more realistically replaced by a modified threshold factor F^G,

$$F^G = \frac{(V^G - a_{G'}^{|G|}v_{G'}^{|G|}N^{G'} - \frac{1}{2}A_{G'}^{|G|}v_{G'}^{|G|}M^{G'} - a_{E'}^{\ddagger E}v_{E'}^E N^{\ddagger E'} - \frac{1}{2}A_{E'}^{\ddagger E}v_{E'}^E M^{\ddagger E'})}{\left((\pi/2)[(v_{G'}^{|G|})^2 + (\phi_{G'}^{|G|})^2](a_{G'}^{|G|}N^{G'} + \frac{1}{2}A_{G'}^{|G|}M^{G'} + a_{E'}^{\ddagger E}N^{\ddagger E'} + \frac{1}{2}A_{E'}^{\ddagger E}M^{\ddagger E'})\right)^{1/2}} ,$$

$$a_{E'}^{\ddagger E} = \frac{1}{2}A_{E'}^{\ddagger E} + B_{E'}^{\ddagger E} . \quad (11)$$

Here, afferent contributions from $N^{\ddagger E}$ long-ranged excitatory fibers, e.g., cortico-cortical neurons, have been added, where $N^{\ddagger E}$ might be on the order of 10% of N^*: Of the approximately 10^{10} to 10^{11} neocortical neurons, estimates of the number of pyramidal cells range from 2/3 up to 4/5 (Markram *et al*, 2004). Nearly every pyramidal cell has an axon branch that makes a cortico-cortical connection; i.e., the number of cortico-cortical fibers is of the order 10^{10}. This development is used in the SMNI description of scalp EEG across regions.

3.4. Centering Mechanism (CM)

It was discovered that more minima of the static Lagrangian $\bar{L}$ are created, i.e., brought into the physical firing ranges, if the numerator of F^G contains terms only in $\bar{M}^G$, tending to center $\bar{L}$ about $\bar{M}^G = 0$ (Ingber, 1984). That is, B^G is modified such that the numerator of F^G is transformed to

$$F'^G = \frac{-\frac{1}{2} A^{|G|}_{G'} v^{|G|}_{G'} M^{G'}}{\mathbf{(}(\pi/2)[(v^{|G|}_{G'})^2 + (\phi^{|G|}_{G'})^2](a'^{|G|}_{G'} N^{G'} + \frac{1}{2} A^{|G|}_{G'} M^{G'})\mathbf{)}^{1/2}} ,$$

$$a'^G_{G'} = \frac{1}{2} A^G_{G'} + B'^G_{G'} , \tag{12}$$

The most likely states of the centered systems lie along diagonals in M^G space, a line determined by the numerator of the threshold factor in F^E, essentially

$$A^E_E M^E - A^E_I M^I \approx 0 , \tag{13}$$

noting that in F^I $I - I$ connectivity is experimentally observed to be very small relative to other pairings, so that $(A^I_E M^E - A^I_I M^I)$ is typically small only for small M^E.

Of course, any mechanism producing more as well as deeper minima is statistically favored. However, this particular CM has plausible support: $M^G(t+\tau) = 0$ is the state of afferent firing with highest statistical weight. I.e., there are more combinations of neuronal firings, $\sigma_j = \pm 1$, yielding this state than any other $M^G(t+\tau)$, e.g., $\approx 2^{N^G+1/2}(\pi N^G)^{-1/2}$ relative to the states $M^G = \pm N^G$. Similarly, $M^G(t)$ is the state of efferent firing with highest statistical weight. Therefore, it is natural to explore mechanisms which favor common highly weighted efferent and afferent firings in ranges consistent with favorable firing threshold factors $F^G \approx 0$.

In general, B^G_E and B^G_I (and possibly A^G_E and A^G_I due to actions of neuromodulators, and J_G constraints from long-ranged fibers) are available to zero the constant in the numerator, giving an extra degree(s) of freedom to this mechanism. (If B'^G_E would be negative, this leads to unphysical results in the square-root denominator of F^G. In all examples where this occurs, it is possible to instead find positive B'^G_I to appropriately shift the numerator of F^G.) In this context, it is empirically observed that the synaptic sensitivity of neurons engaged in selective attention is altered, presumably by the influence of chemical neuromodulators on postsynaptic neurons at their presynaptic sites (Mountcastle *et al*, 1981).

3.5. Prototypical Cases

Three Cases of neuronal firings were considered in the first introduction of STM applications of SMNI (Ingber, 1984). Below is a short summary of these details. Note that while it suffices to define these Cases using F^G, the full Lagrangian and probability distribution, upon which the derivation of the EL equations are based, are themselves quite nonlinear functions of F^G, e.g., via hyperbolic trigonometric functions, etc.

Since STM duration is long relative to τ, stationary solutions of the Lagrangian L, $\bar{L}$, can be investigated to determine how many stable minima $\ll \bar{M}^G \gg$ may simultaneously exist within this duration. Detailed calculations of time-dependent folding of the full time-dependent probability distribution supports persistence of these stable states within SMNI calculations of observed decay rates of STM (Ingber & Nunez, 1995).

A model of dominant inhibition describes how minicolumnar firings are suppressed by their neighboring minicolumns. For example, this could be effected by developing NN mesocolumnar interactions (Ingber, 1983), but here the averaged effect is established by inhibitory mesocolumns (Case I) by setting $A^I_E = A^E_I = 2A^E_E = 0.01N^*/N$. Since there appears to be relatively little $I-I$ connectivity, set $A^I_I = 0.0001N^*/N$. The background synaptic noise is taken to be $B^E_I = B^I_E = 2B^E_E = 10B^I_I = 0.002N^*/N$. As minicolumns are observed to have about 110 neurons (visual cortex appears to have approximately twice this density) (Mountcastle, 1978), and as there appear to be a predominance of E over I neurons (Nunez, 1981), here take $N^E = 80$ and $N^I = 30$. Use $N^*/N = 10^3$, $v^G_{G'}$, and $\phi^G_{G'}$ as estimated previously. $\bar{M}^G$ represents time-averaged M^G. The threshold factors $F^G_{\rm I}$ for this I model are then

$$F^E_{\rm I} = \frac{(0.5\bar{M}^I - 0.25\bar{M}^E + 3.0)}{\pi^{1/2}(0.1\bar{M}^I + 0.05\bar{M}^E + 9.80)^{1/2}} ,$$

$$F^I_{\rm I} = \frac{(0.005\bar{M}^I - 0.5\bar{M}^E - 45.8)}{\pi^{1/2}(0.001\bar{M}^I + 0.1\bar{M}^E + 11.2)^{1/2}} . \tag{14}$$

In the prepoint-discretized deterministic limit, the threshold factors determine when and how smoothly the step-function forms $\tanh F^G_{\rm I}$ in $g^G(t)$ change $M^G(t)$ to $M^G(t+\tau)$. $F^I_{\rm I}$ will cause afferent $\bar{M}^I$ to fire for most of its values, as $\bar{M}^I \approx -N^I \tanh F^I_{\rm I}$ will be positive for most values of $\bar{M}^G$ in $F^I_{\rm I}$, which is already weighted heavily with a term -45.8. Looking at $F^E_{\rm I}$, it is seen that the relatively high positive values of efferent $\bar{M}^I$ require at least moderate values of positive efferent $\bar{M}^E$ to cause firings of afferent $\bar{M}^E$.

The centering effect of the I model, labeled here as the IC model, is quite easy for neocortex to accommodate. For example, this can be accomplished simply by readjusting the synaptic background noise from B^G_E to B'^G_E,

$$B'^G_E = \frac{[V^G - (\frac{1}{2}A^G_I + B^G_I)v^G_I N^I - \frac{1}{2}A^G_E v^G_E N^E]}{v^G_E N^G} \tag{15}$$

for both $G = E$ and $G = I$. In general, B^G_E and B^G_I (and possibly A^G_E and A^G_I due to actions of neuromodulators, and J_G constraints from long-ranged fibers) are available to zero the constant in the numerator, giving an extra degree(s) of freedom to this mechanism. (If B'^G_E would be negative, this leads to unphysical results in the square-root denominator of F^G. In all examples where this occurs, it is possible to instead find positive B'^G_I to appropriately shift the numerator of F^G.) In this context, it is empirically observed that the synaptic sensitivity of neurons engaged in selective attention is altered, presumably by the influence of chemical neuromodulators on postsynaptic neurons at their presynaptic sites (Mountcastle *et al*, 1981).

By this CM, $B'^E_E = 1.38$ and $B'^I_I = 15.3$, and $F^G_{\rm I}$ is transformed to $F^G_{\rm IC}$, Case IC,

$$F^E_{\rm IC} = \frac{(0.5\bar{M}^I - 0.25\bar{M}^E)}{\pi^{1/2}(0.1\bar{M}^I + 0.05\bar{M}^E + 10.4)^{1/2}} ,$$

$$F^I_{\rm IC} = \frac{(0.005\bar{M}^I - 0.5\bar{M}^E)}{\pi^{1/2}(0.001\bar{M}^I + 0.1\bar{M}^E + 20.4)^{1/2}} . \tag{16}$$

Note that, aside from the enforced vanishing of the constant terms in the numerators of $F^G_{\rm I}$, the only other changes in $F^G_{\rm I}$ moderately affect the constant terms in the denominators.

The other extreme of normal neocortical firings is a model of dominant excitation, effected by establishing excitatory mesocolumns (Case E) by using the same parameters $\{B^G_{G'}, v^G_{G'}, \phi^G_{G'}, A^I_I\}$ as in the I model, but setting $A^E_E = 2A^I_E = 2A^E_I = 0.01N^*/N$. This yields

$$F^E_{\rm E} = \frac{(0.25\bar{M}^I - 0.5\bar{M}^E - 24.5)}{\pi^{1/2}(0.05\bar{M}^I + 0.10\bar{M}^E + 12.3)^{1/2}} ,$$

$$F^I_{\rm E} = \frac{(0.005\bar{M}^I - 0.25\bar{M}^E - 25.8)}{\pi^{1/2}(0.001\bar{M}^I + 0.05\bar{M}^E + 7.24)^{1/2}} \ . \tag{17}$$

The negative constant in the numerator of $F^I_{\rm E}$ inhibits afferent $\bar{M}^I$ firings. Although there is also a negative constant in the numerator of $F^E_{\rm E}$, the increased coefficient of $\bar{M}^E$ (relative to its corresponding value in $F^E_{\rm I}$), and the fact that $\bar{M}^E$ can range up to $N^E = 80$, readily permits excitatory firings throughout most of the range of $\bar{M}^E$.

Applying the CM to E, $B'^E_I = 10.2$ and $B'^I_I = 8.62$. The net effect in $F^G_{\rm EC}$, Case EC, in addition to removing the constant terms in the numerators of $F^G_{\rm E}$, is to change the constant terms in the denominators: 12.3 in $F^E_{\rm E}$ is changed to 17.2 in $F^E_{\rm EC}$, and 7.24 in $F^I_{\rm E}$ is changed to 12.4 in $F^I_{\rm EC}$.

Now it is natural to examine a balanced Case intermediate between I and E, labeled here as Case B. This is accomplished by changing $A^E_E = A^I_E = A^E_I = 0.005N^*/N$. This yields

$$F^E_{\rm B} = \frac{(0.25\bar{M}^I - 0.25\bar{M}^E - 4.50)}{\pi^{1/2}(0.050\bar{M}^E + 0.050\bar{M}^I + 8.30)^{1/2}} \ ,$$

$$F^I_{\rm B} = \frac{(0.005\bar{M}^I - 0.25\bar{M}^E - 25.8)}{\pi^{1/2}(0.001\bar{M}^I + 0.050\bar{M}^E + 7.24)^{1/2}} \ . \tag{18}$$

Applying the CM to B, $B'^E_E = 0.438$ and $B'^I_I = 8.62$. The net effect in $F^G_{\rm BC}$, Case BC, in addition to removing the constant terms in the numerators of $F^G_{\rm B}$, is to change the constant terms in the denominators: 8.30 in $F^E_{\rm B}$ is changed to 7.40 in $F^E_{\rm BC}$, and 7.24 in $F^I_{\rm B}$ is changed to 12.4 in $F^I_{\rm BC}$.

Previously, calculations were performed for the three prototypical firing Cases, dominate excitatory (E), dominate inhibitory (I) and balanced about evenly (B). More minima were brought within physical firing ranges when a CM is invoked (Ingber, 1984), by tuning the presynaptic stochastic background, a phenomena observed during selective attention, giving rise to Cases EC, IC and BC. The states BC are observed to yield properties of auditory STM, e.g., the 7 ± 2 capacity rule and times of duration of these memory states (Ingber, 1984; Ingber, 1985c).

It is observed that visual neocortex has twice the number of neurons per minicolumn as other regions of neocortex. In the SMNI model this gives rise to fewer and deeper STM states, consistent with the observed 4 ± 2 capacity rule of these memory states. These calculations are Cases ECV, ICV and BCV (Ingber, 1994).

3.6. Euler-Lagrange (EL)

To investigate dynamics of multivariate stochastic nonlinear systems, such as neocortex presents, it is not sensible to simply apply simple mean-field theories which assume sharply peaked distributions, since the dynamics of nonlinear diffusions in particular are typically washed out. Here, path integral representations of systems, otherwise equivalently represented by Langevin or Fokker-Planck equations, present elegant algorithms by use of variational principles leading to EL equations (Langouche *et al*, 1982).

SMNI permits scaling to derive EL in several approximations which give insight into other phenomena that take advantage of the SMNI STM approach.

3.6.1. Columnar EL

The Lagrangian components and EL equations are essentially the counterpart to classical dynamics,

$$\text{Mass} = g_{GG'} = \frac{\partial^2 L}{\partial(\partial M^G/\partial t)\partial(\partial M^{G'}/\partial t)} \ ,$$

$$\text{Momentum} = \Pi^G = \frac{\partial L}{\partial(\partial M^G/\partial t)} \ ,$$

$$\text{Force} = \frac{\partial L}{\partial M^G} ,$$

$$\text{F} - \text{ma} = 0: \ \delta L = 0 = \frac{\partial L}{\partial M^G} - \frac{\partial}{\partial t} \frac{\partial L}{\partial (\partial M^G/\partial t)} . \tag{19}$$

The EL equations are derived from the long-time conditional probability distribution of columnar firings over all cortex, represented by $\tilde{M}$, in terms of the Action S,

$$\tilde{P}[\tilde{M}(t)] d\tilde{M}(t) = \int \cdots \int D\tilde{M} \exp(-N\tilde{S}) ,$$

$$\tilde{M} = \{M^{G\nu}\} \ , \ \tilde{S} = \int_{t_0}^{t} dt' \tilde{L} \ , \tilde{L} = \Lambda\Omega^{-1} \int d^2 r L \ , \ L = L^E + L^I ,$$

$$D\tilde{M} = \prod_{s=1}^{u+1} \prod_{\nu=1}^{\Lambda} \prod_{G}^{E,I} (2\pi dt)^{-1/2} (g_s^\nu)^{1/4} dM_s^{G\nu} \ \delta[M_t = M(t)][\delta[M_0 = M(t_0)] , \tag{20}$$

where ν labels the two-dimensional laminar $\vec{r}$-space of $\Lambda \approx 5 \times 10^5$ mesocolumns spanning a typical region of neocortex, Ω, (total cortical area $\approx 4 \times 10^{11}$ μm^2); and s labels the $u+1$ time intervals, each of duration $dt \leq \tau$, spanning $(t - t_0)$. At a given value of $(r; t)$, $M = \{M^G\}$.

The path integral has a variational principle, $\delta L = 0$ which gives the EL equations for SMNI (Ingber, 1982; Ingber, 1983). The Einstein convention is used to designate summation over repeated indices, and the following notation for derivatives is used:

$$(\cdots)_{:z} \ = d(\cdots)/dz, \ \ z = \{x, y\} ,$$

$$(\cdots)_{,G} \ = \partial(\cdots)/\partial M^G, \ \ (\cdots)_{,\dot{G}} = \partial(\cdots)/\partial(dM^G/dt),$$

$$(\cdots)_{,G_{:z}} = \partial(\cdots)/\partial(dM^G/dz),$$

$$(\cdots)_{,\nabla G} = \hat{x}\partial(\cdots)/\partial(dM^G/dx) + \hat{y}\partial(\cdots)/\partial(dM^G/dy). \tag{21}$$

The EL equations are:

$$\delta L \ \ = 0,$$

$$\delta_G L \ \ = L_{,G} - \nabla \cdot L_{,\nabla G} - L_{,\dot{G}:t} = 0,$$

$$\nabla \cdot L_{,\nabla G} = L_{,G_{:z}:z} = (L_{,G_{:z}\,,G'}) M^{G'}{}_{:z} + (L_{,G_{:z}\,,G'_{:z}}) M^{G'}{}_{:zz}$$

$$L_{,\dot{G}:t} = (L_{,\dot{G}\,,G'}) \dot{M}^{G'} + (L_{,\dot{G}\,,\dot{G}'}) \ddot{M}^{G'} . \tag{22}$$

This exhibits the extremum condition as a set of differential equations in the variables $\{M^G, \dot{M}^G, \ddot{M}^G, M^G{}_{:z}, M^G{}_{:zz}\}$ in $r - t = (x, y, t)$ space, with coefficients nonlinear in M^G. Note that the V' term for NN interactions in the Lagrangian L will introduce spatial derivative terms that appear in these EL equations.

As noted above, linearization of the EL equations permit the development of stability analyses and dispersion relations in frequency-wave-number space (Ingber, 1982; Ingber, 1983; Ingber, 1985b), leading to wave propagation velocities of interactions over several minicolumns, consistent with experiments. This calculation first linearizes the EL, then takes Fourier transforms in space and time variables.

$$M^G = \text{Re} \ M^G_{\text{osc}} \exp[-i(\xi \cdot r - \omega t)] ,$$

$$M^G_{\text{osc}}(r, t) = \int d^2\xi d\omega \ \hat{M}^G_{\text{osc}}(\xi, \omega) \exp[i(\xi \cdot r - \omega t)] . \tag{23}$$

For instance, a typical example (Ingber, 1985b). is specified by: extrinsic sources (used in earlier papers as a centering mechanism) $J_E = -2.63$ and $J_I = 4.94$, $N^E = 125$, $N^I = 25$, $V^G = 10$ mV, $A^E = 1.75$, $A^I = 1.25$, $B^G = 0.25$, $v^G 0.1$ mv, and $\phi^G = 0.03^{1/2}$ mV. The global minima is at $\bar{M}^E = 25$ and $\bar{M}^I = 5$. This set of conditions yields (dispersive) dispersion relations

$$\omega\tau = \pm\{-1.86 + 2.38(\xi\rho)^2; -1.25i + 1.51i(\xi\rho)^2\}\ , \tag{A8}$$

where $\xi = |\xi|$. The propagation velocity defined by $d\omega/d\xi$ is about 1 cm/sec, taking typical wave-numbers ξ to correspond to macrocolumnar distances about 30ρ. Calculated frequencies ω are on the order of EEG frequencies of about 10^2 sec^{-1}. These mesoscopic propagation velocities permit processing over several minicolumns about 10^{-1} cm, simultaneous with processing of mesoscopic interactions over tens of cm via association fibers with propagation velocities about 600—900 cm/sec. I.e., both can occur within about 10^{-1} sec.

Note that this propagation velocity is not ''slow'': Visual selective attention moves at about 8 msec/degree (Tsal, 1983), which is about 1/2 mm/sec, if a macrocolumn of about mm^2 is assumed to span 180 degrees. This suggests that NN interactions play some part in disengaging and orienting selective attention.

3.6.2. Strings EL

The nonlinear string model was derived using the EL equation for the electric potential Φ measured by EEG, considering one firing variable along the parabolic trough of attractor states being proportional to Φ (Ingber & Nunez, 1990).

Since only one variable, the electric potential is being measured, is reasonable to assume that a single independent firing variable offers a crude description of this physics. Furthermore, the scalp potential Φ can be considered to be a function of this firing variable. (Here, "potential" refers to the electric potential, not any potential term in the SMNI Lagrangian.) In an abbreviated notation subscripting the time-dependence,

$$\Phi_t - \ll \Phi \gg = \Phi(M_t^E, M_t^I) \approx a(M_t^E - \ll M^E \gg) + b(M_t^I - \ll M^I \gg)\ , \tag{24}$$

where a and b are constants, and $\ll \Phi \gg$ and $\ll M^G \gg$ represent typical minima in the trough. In the context of fitting data to the dynamic variables, there are three effective constants, $\{\ a, b, \phi\ \}$,

$$\Phi_t - \phi = aM_t^E + bM_t^I \tag{25}$$

The mesoscopic columnar probability distributions, P, is scaled over this columnar firing space to obtain the macroscopic conditional probability distribution over the scalp-potential space:

$$P_\Phi[\Phi] = \int dM^E dM^I P[M^E, M^I]\delta[\Phi - \Phi'(M^E, M^I)] \tag{26}$$

The parabolic trough described above justifies a form

$$P_\Phi = (2\pi\sigma^2)^{-1/2} \exp(-\Delta t \int dx\, L_\Phi)\ ,$$

$$L_\Phi = \frac{\alpha}{2}|\partial\Phi/\partial t|^2 + \frac{\beta}{2}|\partial\Phi/\partial x|^2 + \frac{\gamma}{2}|\Phi|^2 + F(\Phi)\ ,$$

$$\sigma^2 = 2\Delta t/\alpha\ , \tag{27}$$

where $F(\Phi)$ contains nonlinearities away from the trough, σ^2 is on the order of $1/N$ given the derivation of L above, and the integral over x is taken over the spatial region of interest. In general, there also will be terms linear in $\partial\Phi/\partial t$ and in $\partial\Phi/\partial x$.

Here, the EL equation includes variation across the spatial extent, x, of columns in regions,

$$\frac{\partial}{\partial t}\frac{\partial L}{\partial(\partial\Phi/\partial t)} + \frac{\partial}{\partial x}\frac{\partial L}{\partial(\partial\Phi/\partial x)} - \frac{\partial L}{\partial\Phi} = 0 \tag{28}$$

The result is

$$\alpha \frac{\partial^2 \Phi}{\partial t^2} + \beta \frac{\partial^2 \Phi}{\partial x^2} + \gamma \Phi - \frac{\partial F}{\partial \Phi} = 0 \tag{29}$$

The determinant prefactor g defined above also contains nonlinear details affecting the state of the system. Since g is often a small number, distortion of the scale of L is avoided by normalizing g/g_0, where g_0 is simply g evaluated at $M^E = M^{\ddagger E'} = M^I = 0$.

If there exist regions in neocortical parameter space such that $\beta/\alpha = -c^2$, $\gamma/\alpha = \omega_0^2$, i.e., as explicitly calculated using the Centering Mechanism (CM) and as derived in previous SMNI EEG papers,

$$\frac{1}{\alpha} \frac{\partial F}{\partial \Phi} = -\Phi f(\Phi) , \tag{30}$$

then the nonlinear string model is recovered.

Note that if the spatial extent is extended across the scalp via long-ranged fibers connecting columns with $M^{\ddagger E'}$ firings, this leads to a string of columns.

3.6.3. Springs EL

For a given column in terms of the probability description given above, the above EL equations are represented as

$$\frac{\partial}{\partial t} \frac{\partial L}{\partial (\partial M^E/\partial t)} - \frac{\partial L}{\partial M^E} = 0 ,$$

$$\frac{\partial}{\partial t} \frac{\partial L}{\partial (\partial M^I/\partial t)} - \frac{\partial L}{\partial M^I} = 0 \tag{31}$$

Previous SMNI EEG studies had demonstrated that simple linearized dispersion relations derived from the EL equations support the local generation of frequencies observed experimentally as well as deriving diffusive propagation velocities of information across minicolumns consistent with other experimental studies. Then, the above equations can represent coupled springs. The earliest studies simply used a driving force $J_G M^G$ in the Lagrangian to model long-ranged interactions among fibers (Ingber, 1982; Ingber, 1983). Subsequent studies considered regional interactions driving localized columnar activity within these regions (Ingber, 1996b; Ingber, 1997; Ingber, 1998).

A recent set of calculations examined these columnar EL equations to see if EEG oscillatory behavior could be supported at just this columnar scale, i.e., within a single column. At first, the EL equations were quasi-linearized, by extracting coefficients of M and dM/dt. The nonlinear coefficients were presented as graphs over all firing states (Ingber, 2009a). This exercise demonstrated that a spring-type model of oscillations was plausible. Then a more detailed study was performed, developing over two million lines of C code from the algebra generated by an algebraic tool, Maxima, to see what range of oscillatory behavior could be considered as optimal solutions satisfying the EL equations (Ingber, 2009b). The answer was affirmative, in that ranges of $\omega t \approx 1$ were supported, implying that oscillatory solutions might be sustainable just due to columnar dynamics at that scale. The full probability distribution was evolved with such oscillatory states, confirming this is true.

These results survive even with oscillatory input into minicolumns from long-ranged sources (Ingber & Nunez, 2010), since the CM is independent of firing states, and just depends on averaged synaptic values used in SMNI.

3.7. Computational Physics

3.7.1. Adaptive Simulated Annealing (ASA)

Adaptive Simulated Annealing (ASA) (Ingber, 1993) is used to optimize or importance-sample parameters of systems.

ASA is a C-language code developed to statistically find the best global fit of a nonlinear constrained non-convex cost-function over a D-dimensional space. This algorithm permits an annealing schedule for

"temperature" T decreasing exponentially in annealing-time k, $T = T_0 \exp(-ck^{1/D})$. The introduction of re-annealing also permits adaptation to changing sensitivities in the multi-dimensional parameter-space. This annealing schedule is faster than fast Cauchy annealing, where $T = T_0/k$, and much faster than Boltzmann annealing, where $T = T_0/\ln k$. ASA has over 100 OPTIONS to provide robust tuning over many classes of nonlinear stochastic systems (Ingber, 2012).

For example, ASA has ASA_PARALLEL OPTIONS, hooks to use ASA on parallel processors, which were first developed in 1994 when the author was Principal Investigator (PI) of a National Science Foundation grant, Parallelizing ASA and PATHINT Project (PAPP). Since then these OPTIONS have been used by people in various institutions.

3.7.2. PATHINT and PATHTREE

In some cases, it is desirable to develop a time evolution of a short-time conditional probability. Two useful algorithms have been developed and published by the author.

PATHINT (Ingber, 1994) motivated the development of PATHTREE (Ingber, Chen *et al*, 2001), an algorithm that permits extremely fast accurate computation of probability distributions of a large class of general nonlinear diffusion processes.

The natural metric of the space is used to first lay down the mesh. The evolving local short-time distributions on this mesh are then dynamically calculated. The short-time probability density gives the correct result up to order $O(\Delta t)$ for any final point S', the order required to recover the corresponding partial differential equation. In fact, $O(\Delta t^{3/2})$ is available (Graham, 1978; Langouche *et al*, 1979; Langouche *et al*, 1982).

PATHINT and PATHTREE have demonstrated their utility in statistical mechanical studies in finance, neuroscience, combat analyses, neuroscience, and other selected nonlinear multivariate systems (Ingber, Fujio & Wehner, 1991; Ingber & Nunez, 1995; Ingber, 2000). PATHTREE has been used extensively to price financial options (Ingber, Chen *et al*, 2001).

3.8. Generic Mesoscopic Neural Networks (MNN)

SMNI was applied to a parallelized generic mesoscopic neural networks (MNN) (Ingber, 1992), adding computational power to a similar paradigm proposed for target recognition (Ingber, 1985a).

"Learning" takes place by presenting the MNN with data, and parameterizing the data in terms of the firings, or multivariate firings. The "weights," or coefficients of functions of firings appearing in the drifts and diffusions, are fit to incoming data, considering the joint "effective" Lagrangian (including the logarithm of the prefactor in the probability distribution) as a dynamic cost function. This program of fitting coefficients in Lagrangian uses methods of ASA.

"Prediction" takes advantage of a mathematically equivalent representation of the Lagrangian path-integral algorithm, i.e., a set of coupled Langevin rate-equations. A coarse deterministic estimate to "predict" the evolution can be applied using the most probable path, but PATHINT has been used. PATHINT, even when parallelized, typically can be too slow for "predicting" evolution of these systems. However, PATHTREE is much faster.

3.9. Ideas by Statistical Mechanics (ISM)

These kinds of applications of SMNI have obvious counterparts in an AI approach to Ideas by Statistical Mechanics (ISM). ISM is a generic program to model evolution and propagation of ideas/patterns throughout populations subjected to endogenous and exogenous interactions (Ingber, 2006; Ingber, 2007; Ingber, 2008). The program is based on SMNI, and uses the ASA code (Ingber, 1993) for optimizations of training sets, as well as for importance-sampling to apply the author's copula financial risk-management codes, TRD (Ingber, 2005; Ingber, 2010), for assessments of risk and uncertainty. This product can be used for decision support for projects ranging from diplomatic, information, military, and economic (DIME) factors of propagation/evolution of ideas, to commercial sales, trading indicators across sectors of financial markets, advertising and political campaigns, etc.

It seems appropriate to base an approach for propagation of ideas on the only system so far demonstrated to develop and nurture ideas, i.e., the neocortical brain. Ultimately, ISM of course would not use functional relationships developed solely in neocortex, but rather those more appropriate to a given population. Following the SMNI structure, ISM develops subsets of macrocolumnar activity of multivariate stochastic descriptions of defined populations, with macrocolumns defined by their local parameters within specific regions and with parameterized endogenous inter-regional and exogenous external connectivities. Parameters of subsets of macrocolumns are to be fit using ASA to patterns representing ideas. Parameters of external and inter-regional interactions are to be determined that promote or inhibit the spread of these ideas.

4. Top-Down Versus Bottom-Up

In regard to neocortical information processing at the level of STM, there are two major paradigms that have not yet been reconciled, which is conveniently understood in terms of top-down versus bottom-up processes.

4.1. Bottom Up

There has been much work done, both experimentally and theoretically, detailing quite a few specific mechanisms at the level of individual neurons and glial processes and their interactions, that can explain information processing and codification of information that may be instrumental in STM (Amzica & Massimini, 2002). In particular, a class of glial cells, astrocytes, present in numbers greater than neurons in human neocortex, is of interest here (Oberheim *et al*, 2009). For example, astrocytes in neocortical laminae 1 extend their mm processes across associative/computing laminae 1-3, afferent laminae 4, touching and communicating with other glia cells and neurons (Reisin & Colombo, 2002; Colombo *et al*, 2005). Laminae 2-6 have larger astrocytes, and in laminae 5-6 with mostly efferent neuronal processes there are some astrocytes with varicose projections (Oberheim *et al*, 2009). However, it appears that a primary means of communication among astrocytes (and other glial cells) is via Ca^{2+} waves, propagating at speeds up to 40 μm/s (Bellinger, 2005) over hundreds of mm of neuronal structures. They influence excitation and inhibition of neuromodulators, and recent research points to their direct effect on polarization thresholds via Ca^{2+} waves. For example, the influence of neuron firing on astroglial calcium ions may be caused by movement of sodium and potassium ions in and out the body and axon of neurons.

It should be noted that there are other mechanisms proposed, other than direct neuron-neuron interactions, to describe various aspects of neocortical information processing, e.g., soliton formation (Georgiev, 2003), and ephaptic excitation of neurons (Anastassiou *et al*, 2011).

There are many approaches in this "bottom-up" context, including quantum computation in microtubles (Hagan *et al*, 2002), nonlinear systems approaches to neural processes (Rabinovich *et al*, 2006), magnetic processes within astrocytes (Banaclocha, 2005; Banaclocha, 2007; Banaclocha & Banaclocha, 2010; Banaclocha, Bóokkon & Banaclocha, 2010), pulsating Ca^{2+} waves in astrocytes (Schipke *et al*, 2002; Scemes *et al*, 2000; Goldberg *et al*, 2010), neuron-astrocyte networks (Pereira & Furlan, 2009; Pereira & Furlan, 2010), including glutamate-specific Ca^{2+}-induced signaling processes between neurons and astrocytes (Postnov *et al*, 2009), influences of blood flow on neuronal processes (Moore & Cao, 2008), and mathematical formulations of qualia based on neural information processing (Balduzzi & Tononi, 2009).

4.2. Top Down

There has been much theoretical work done at the level of columnar and regional neocortical activity, detailing correlations of experimental brain activity with behavioral observations (Buxhoeveden & Casanova, 2002; Rakic, 2008). For example, various imaging techniques, both intra-cranial and non-invasive, have demonstrated that specific brain activity often is correlated with STM as well as specific processing of information and attentional states (Nunez & Srinivasan, 2006).

There also has been much theoretical work trying to bridge brain activity across multiples scales, e.g., from neuronal to columnar to regional scales of activity, with detailed calculations defining STM (Ingber, 1981; Ingber, 1983; Ingber, 1984; Ingber & Nunez, 1995) and analyses of scalp EEG (Ingber, 1997; Ingber, 2009b; Ingber & Nunez, 2010). Using SMNI, minicolumnar EEG has been demonstrated to scale

up to EEG observed at regional scalp measurements. While minicolumnar EEG may not be the only source of scalp EEG, it is sufficient to scale for detailed fits to observed scalp EEG data.

It is reasonable to state that, while most neuroscientists believe that ultimately Bottom Up processing will explain all brain activity (Rabinovich *et al*, 2006), some other neurophysiologists and psychologists believe that direct Top Down processes are important components of mammalian information processing, which cannot be solely explained by Bottom Up processes.

4.2.1. Smoking Gun

As yet, there does not seem to be any "smoking gun" for explicit Top to Down mechanisms that directly drive Bottom Up STM processes. Of course, there are many Top Down type studies demonstrating that neuromodulator (Silberstein, 1995) and neuronal firing states, e.g., as defined by EEG frequencies, can modify the milieu or context of individual synaptic and neuronal activity, which is still consistent with ultimate Bottom Up paradigms. However, there is a logical difference between Top Down milieu as conditioned by some prior external or internal conditions, and some direct Top Down processes that direct cause Bottom Up interactions specific to STM. Here, the operative word is "cause".

4.3. Support for Top-Down Electromagnetic Mechanism

There is a body of evidence that suggests a specific Top to Down mechanism for neocortical STM processing.

4.3.1. Magnetism Influences in Living Systems

An example of a direct physical mechanism that affects neuronal processing not part of "standard" sensory influences is the strong possibility of magnetic influences in birds at quantum levels of interaction (Kominis, 2009; Rodgers & Hore, 2009; Solov'yov & Schulten, 2009). It should be noted that this is just a proposed mechanism (Johnsen & Lohmann, 2008).

4.3.2. Neocortical Magnetic Fields

There are many studies on electric (Alexander *et al*, 2006) and magnetic fields in neocortex (Murakami & Okada, 2006; McFadden, 2007; Irimia *et al*, 2009; Georgiev, 2003).

At the level of a single neuron, electric field strengths can be as high as about 10V/m for a summation of excitatory or inhibitory postsynaptic potentials as a neuron fires. The electric field **D**

$$\mathbf{D} = \varepsilon \mathbf{E} \tag{32}$$

is rapidly attenuated as the dielectric constant ε seen by ions is close to two orders of magnitude times that in vacuum, ε_0 due to polarization of water (Nunez, 1981). Magnetic field strengths **H** in neocortex are generally quite small, even when estimated for the largest human axons at about 10^{-7}T, about 1/300 of the Earth's magnetic field, based on ferrofluid approximation to the microtuble environment with a magnetic permeability μ,

$$\mathbf{B} = \boldsymbol{\mu} \mathbf{H} \tag{33}$$

about $10\mu_0$ (Georgiev, 2003). Thus, the electromagnetic fields in neocortex differ substantially from those in vacuum, i.e.,

$$\varepsilon_0 \mu_0 c^2 = 1 \tag{34}$$

where c is the speed of light. These estimates of magnetic field strengths appear to be reliable when comparisons between theoretical and experimental measurements are made in crayfish axons (Roth & Wikswo, 1985).

The above estimates of electric and magnetic field strengths do not consider collective interactions within and among neighboring minicolumns, which give rise to field strengths much larger as typically measured by noninvasive EEG and MEG recordings. While electrical activity may be attenuated in the neocortical environment, this is not true for magnetic fields which may increase collective strengths over relatively large neocortical distances. The strengths of magnetic fields in neocortex may be at a threshold to

directly influence synaptic interactions with astrocytes, as proposed for long-term memory (LTM) (Gordon *et al*, 2009) and short-term memory (STM) (Banaclocha, 2007; Pereira & Furlan, 2010) Magnetic strengths associated by collective EEG activity at a columnar level gives rise to even stronger magnetic fields. Columnar excitatory and inhibitory processes largely take place in different neocortical laminae, providing possibilities for more specific mechanisms.

4.3.3. Columnar EEG

Details of STM have been calculated in the SMNI papers. The Centering Mechanism (CM), associated in these calculations with changes in background inhibitory synaptic activity, drive the columnar system into multiple collective firing states. This CM leads to detailed calculations of STM capacity, duration and stability that agrees with experimental observations.

Future work must consider magnetic fields produced at different laminae due to collective minicolumnar firings as detailed by SMNI for STM processes. These magnetic fields may affect Ca^{2+} ion waves that are considered by some researchers as being vital processes for astrocyte-neural interactions that give rise to higher-order cognitive states (Bellinger, 2005; Nakano *et al*, 2007).

The interactions between the momentum of these Ca^{2+} ions and minicolumnar magnetic fields can be approached classically, e.g., at a local minicolumnar scale, or quantum mechanically, e.g., considering possible entanglement across macrocolumnar scales.

4.4. Bottom-Up Complementary to SMNI STM

It is essential to recognize that, while SMNI STM has done well in calculating properties of STM, neuronal firing states are likely the just first fast stages of STM, and it must be appreciated that other molecular mechanisms are likely essential to understanding just how STM and LTM are processed and stored in some kind of coded neuronal-glial states.

A particularly plausible set of mechanisms has been proposed that reply on specific bio-magnetic processes among neurons and astrocytes (Banaclocha, Bóokkon & Banaclocha, 2010; Banaclocha, 2011). This proposal is that neurons synthesize and accumulate predominantly superparamagnetic magnetite, while astrocytes generate and accumulate preferentially single-domain magnetite nano-particles which have a permanent magnetic moment. This set of interacting mechanisms can plausibly code both STM and LTM. These mechanisms propose collective minicolumnar neuronal activity as possibly generating strong enough magnetic fields. Also, collective Ca^{2+} waves are invoked that may generate strong enough magnetic processes to develop astrocyte magnetic bubbles. These bubbles are a key concept in this proposal for processing information.

The section below on Vector Potential further details how SMNI STM can interface with electromagnetic processes affecting neuron-astrocyte interactions.

5. Vector Potential

To demonstrate that top-down influences can be appreciable, here a direct comparison is described between the momentum $\mathbf{p}$ of Ca^{2+}, ions which already have been established as being influential in STM and LTM, and an SMNI vector potential (SMNI-VP). The SMNI-VP is constructed from magnetic fields induced by neuronal electrical firings, at thresholds of collective minicolumnar activity with laminar specification, can give rise to causal top-down mechanisms that effect molecular excitatory and inhibitory processes in STM and LTM. A specific example might be causal influences on momentum $\mathbf{p}$ of Ca^{2+} ions by the SMNI-VP $\mathbf{A}$, as calculated by the canonical momentum $\mathbf{q}$

$$\mathbf{q} = \mathbf{p} - q\mathbf{A} \tag{35}$$

where $q = -2e$ for Ca^{2+}, e is the electron coulomb charge and $\mathbf{B} = \nabla \times \mathbf{A}$ is the magnetic field $\mathbf{B}$, which may be applied either classically or quantum-mechanically. Note that gauge of $\mathbf{A}$ is not specified here, and this can lead to important effects especially at quantum scales (Tollaksen *et al*, 2010).

$\mathbf{A}$ can be calculated using the standard assumption that large-scale EEG is developed from oscillatory electrical dipole activity $\mathbf{p}\exp(-i\omega t)$, the first moment of the charge distribution density ρ giving rise to the dipole. The electromagnetic vector potential $\mathbf{A}$ (Jackson, 1962) is

$$\mathbf{A} = \frac{e^{i\omega r/c}}{cr} \int \mathbf{J} d^3x \tag{36}$$

for the electric current density **J**, which in the dipole approximation,

$$\mathbf{p} = \int \mathbf{x}\rho(\mathbf{x}) d^3x \tag{37}$$

gives rise to

$$\mathbf{A} = -\frac{i\omega \mathbf{p} e^{i\omega r/c}}{cr} \tag{38}$$

This is a dipole model for collective minicolumnar oscillatory currents, corresponding to top-down signaling, flowing in axons, not for individual neurons. The top-down signal is claimed to cause relevant effects on the surrounding milieu, but is not appropriate outside these surfaces due to strong attenuation of electrical activity. However, the vector potentials produced by these dipoles due to axonal discharges do survive far from the axons, and this can lead to important effects at the molecular scale, e.g., in the environment of ions (Feynman *et al*, 1964; Giuliani, 2010).

Note that this is not necessarily the only or most popular description of electromagnetic influences in neocortex, which often describes dendritic presynaptic activity as inducing large scale EEG (Nunez, 1981), or axonal firings directly affecting astrocyte processes (McFadden, 2007). This work is only and specifically concerned with electromagnetic fields in collective axonal firings, directly associated with columnar STM phenomena in SMNI calculations, which create vector potentials influencing ion momenta just outside minicolumnar structures.

After fitting the electrical dipole moment **p** to minicolumnar electrical field near minicolumns, this value of **A** is then to be compared to the value of **p** for Ca^{2+}. Note that the magnetic field **B** derived from **A**,

$$\mathbf{B} = \nabla \times \mathbf{A} \tag{39}$$

is still attenuated in the glial areas where Ca^{2+} waves exist, but **A** derived near the minicolumns will be used there as well since it is not so attenuated.

The electrical dipole for collective minicolumnar EEG derived from **A** is

$$\mathbf{E} = \frac{ic}{\omega} \nabla \times \mathbf{B} = \frac{ic}{\omega} \nabla \times \nabla \times \mathbf{A} \tag{40}$$

which in a near-field approximation for minicolumns gives

$$\mathbf{E} = \frac{3\mathbf{n}(\mathbf{n} \cdot \mathbf{p}) - \mathbf{p}}{r^3}$$

$$\mathbf{B} = \frac{i\omega \mathbf{n} \times \mathbf{p}}{cr^2} \tag{41}$$

where **n** is the unit vector in the direction of **p**. The far-field approximations are

$$\mathbf{E} = \mathbf{B} \times \mathbf{n}$$

$$\mathbf{B} = \frac{\omega^2 \mathbf{n} \times \mathbf{p} e^{i\omega r/c}}{(cr)^2} \tag{42}$$

The SMNI columnar probability distributions, derived from statistical aggregation of synaptic and neuronal interactions among minicolumns and macrocolumns, have established credibility at columnar scales by detailed calculations of properties of STM. Under CM conditions, they exhibit multiple columnar collective firing states. It must be stressed that these minicolumns are the entities which the above dipole moment is modeling. The Lagrangian of the SMNI distributions, although possessing multivariate nonlinear means and covariance, have functional forms similar to arguments of firing distributions of individual neurons, so that the description of the columnar dipole above is a model faithful to the standard derivation of a vector potential from an oscillating electric dipole.

The effective collective minicolumnar potential is estimated to be about 10 times as strong as a neuronal postsynaptic voltage of $10^{-3}V$, or 10^{-2} V, where V measures volts, equivalent to m^2-kg-/A-s^3 (A measures amperes). At a laminar thickness, r, within axons, of about 10^{-3} m, the **E** field density dimension is on the order of $10^{-2}/r$ V/m. This gives a dipole value on the order of $10^{-2}r^2$ C-m (C measures coulomb, measured by A-s) at the near field.

This yields an estimate for values of $|\mathbf{A}|$, for $\omega = 6.366$ cps, corresponding to EEG frequencies of 40 s^{-1} A-s/m^2, on the order of $10^{-10}r$ V-m at the near field of firing minicolumns. In SI units, as can be described by the Coulomb force, the equivalent units of C = (kg-$m^3/s^2)^{1/2}$, or eA will be in units of linear momentum. Taking r to be a laminae thickness gives an estimate of 10^{-13} V-m, which decreases as $1/r$ away from the near field, all measured within axons for the purposes of describing electrical activity.

The contribution of **A** to the canonical momentum is measured by $e\mathbf{A}$, where $e = 1.602 \times 10^{-19}$ C. This gives a momentum contribution from **A** on the order of 10^{-32} kg-m/s.

The mass of a Ca^{2+} ion is 6.6×10^{-26} kg. Assuming speeds of 40 μm/s, estimate the momentum of a single ion is estimated to be about 5×10^{-30} kg-m/s.

This comparison of **p** and **A** demonstrates it is possible for minicolumnar electromagnetic fields to influence important ions involved in cognitive and affective processes in neocortex. Our estimate of minicolumnar electric dipole is quite conservative, and a factor of 10 would make these effects even more dramatic. Since this effect acts on all Ca^{2+} ions, it may have an even greater effect on Ca^{2+} waves, contributing to their mean wave-front movement. Considering slower ion momenta **p** would make this comparison to **A** even closer.

Such a smoking gun for top-down effects awaits forensic in vivo experimental verification, requiring appreciating the necessity and due diligence of including true multiple-scale interactions across orders of magnitude in the complex neocortical environment.

6. Conclusion

For several decades the stated Holy Grail of chemical, biological and biophysical research into neocortical information processing has been to reduce such neocortical phenomena into specific bottom-up molecular and smaller-scale processes (Rabinovich *et al*, 2006). Over the past three decades, with regard to short-term memory (STM) and long-term memory (LTM) phenomena, which themselves are likely components of other phenomena like attention and consciousness, the SMNI approach has yielded specific details of STM capacity, duration and stability not present in molecular approaches, but it is clear that most molecular approaches consider it inevitable that their reductionist approaches at molecular and possibly even quantum scales will yet prove to be causal explanations of such phenomena. The SMNI approach is a bottom-up aggregation from synaptic scales to columnar and regional scales of neocortex, and has been merged with larger non-invasive EEG scales with other colleagues -- all at scales much coarser than molecular scales. As with many Crusades for some truths, other truths can be trampled. It is proposed that an SMNI vector potential (SMNI-VP) constructed from magnetic fields induced by neuronal electrical firings, at thresholds of collective minicolumnar activity with laminar specification, can give rise to causal top-down mechanisms that effect molecular excitatory and inhibitory processes in STM and LTM. Such a smoking gun for top-down effects awaits forensic in vivo experimental verification, requiring appreciating the necessity and due diligence of including true multiple-scale interactions across orders of magnitude in the complex neocortical environment.

This work simply shows that electromagnetic fields within neurons can have effects outside of them, e.g., on ions that mediate interactions between and among neurons and astrocytes (Pereira & Furlan, 2010; Pereira & Furlan, 2009). Other work has shown the important computational effects of such interactions, including consideration of magnetic influences per se (Banaclocha, 2007; Banaclocha, Bóokkon & Banaclocha, 2010).

These minicolumnar processes of STM, as described by SMNI, as they affect and are affected by relatively regional macroscopic processes, and as they affect and are affected by relatively microscopic ionic processes, will be emphasized in other papers (Ingber, 2011).

Acknowledgments

I thank Alfredo Pereira Jr and Marcos Banaclocha for several discussions and for references to relevant literature on astrocyte processes. I thank Paul Nunez for several discussions on electrical and magnetic fields in neocortex.

References

Alexander, J.K., Fuss, B. & Colello, R.J. (2006) Electric field-induced astrocyte alignment directs neurite outgrowth. Neuron Glia Biology. 2(2), 93-103.

Amzica, F. & Massimini, M. (2002) Glial and neuronal interactions during slow wave and paroxysmal activities in the neocortex. Cerbral Cortex. 12(10), 1101-1113.

Anastassiou, C.A., Perin, R., Markram, H. & Koch, C. (2011) Ephaptic coupling of cortical neurons. Nature Neuroscience. 14, 217-223.

Balduzzi, D. & Tononi, G. (2009) Qualia: The geometry of integrated information. PLoS Computational Biology. 5(8), 1-24.

Banaclocha, M.A.M. (2005) Magnetic storage of information in the human cerebral cortex: A hypothesis for memory. International Journal of Neuroscience. 115(3), 329-337.

Banaclocha, M.A.M. (2007) Neuromagnetic dialogue between neuronal minicolumns and astroglial network: A new approach for memory and cerebral computation. Brain Research Bulletin. 73, 21-27.

Banaclocha, M.A.M. (2011) Magnetic bubbles in brain neocortex: a new model for neuro-cognitive functions. Report. Hospital Lluis Alcanyis.

Banaclocha, M.A.M. & Banaclocha, H.M. (2010) Spontaneous neocortical activity and cognitive functions: A neuron-astroglial bio-magnetic and self-organized process. NeuroQuantology. 8(2), 191-199.

Banaclocha, M.A.M., Bóokkon, I. & Banaclocha, H.M. (2010) Long-term memory in brain magnetite. Medical Hypotheses. 74(2), 254-257.

Bellinger, S. (2005) Modeling calcium wave oscillations in astrocytes. Neurocomputing. 65(66), 843-850.

Boyd, I.A. & Martin, A.R. (1956) The end-plate potential in mammalian muscle. Journal of Physiology (London). 132, 74-91.

Buxhoeveden, D.P. & Casanova, M.F. (2002) The minicolumn hypothesis in neuroscience. Brain. 125(5), 935-951. [URL http://tinyurl.com/bc2002brain]

Caillé, A., Pink, D., de Verteuil, F. & Zuckermann, M.J. (1980) Theoretical models for quasi-two-dimensional mesomorphic monolayers and membrane bilayers. Canadian Journal of Physics. 58, 1723-1726.

Colombo, J.A., Reisin, H.D., Jones, M. & Bentham, C. (2005) Development of interlaminar astroglial processes in the cerebral cortex of control and Down's syndrome human cases. Experimental Neurology. 193, 207-217.

Cowan, J.D. (1982) Spontaneous symmetry breaking in large scale nervous activity. International Journal of Quantum Chemistry. 22, 1059-1082.

Cragg, B.G. & Temperley, H.N.V. (1954) The organization of neurons: A cooperative analogy. Electroencephalography Clinical Neurophysiology. 6, 85-92.

Ericsson, K.A. & Chase, W.G. (1982) Exceptional memory. American Scientist. 70, 607-615.

Feynman, R.P., Leighton, R.B. & Sands, M. (1964) Chapter 15: The Vector Potential, In: The Feynman Lectures on Physics, Addison-Wesley, 1-16.

Georgiev, D. (2003) Electric and magnetic fields inside neurons and their impact upon the cytoskeletal microtubules. Cogprints Report. Cogprints. [http://cogprints.org/3190/]

Giuliani, G. (2010) Vector potential, electromagnetic induction and 'physical meaning'. European Journal of Physics. 31(4), 871-880.

Goldberg, M., Pittà, M. De, Volman, V., Berry, H. & Ben-Jacob, E. (2010) Nonlinear Gap Junctions Enable Long-Distance Propagation of Pulsating Calcium Waves in Astrocyte Networks. PLoS Computational Biology. 6(8), 1-14.

Gordon, G.R.J., Iremonger, K.J., Kantevari, S., Ellis-Davies, G.C.R., MacVicar, B.A. & Bains, J.S. (2009) Astrocyte-mediated distributed plasticity at hypothalamic glutamate synapses. Neuron. 64, 391-403.

Graham, R. (1977) Covariant formulation of non-equilibrium statistical thermodynamics. Zeitschrift für Physik. B26, 397-405.

Graham, R. (1978) Path-integral methods in nonequilibrium thermodynamics and statistics, In: Stochastic Processes in Nonequilibrium Systems, ed. L. Garrido, P. Seglar & P.J. Shepherd. Springer, 82-138.

Hagan, S., Hameroff, R. & Tuszyński, J.A. (2002) Quantum computation in brain microtubules: Decoherence and biological feasibility. Physical Review E. 65(061901), 1-11.

Hick, W. (1952) On the rate of gains of information. Quarterly Journal Experimental Psychology. 34(4), 1-33.

Ingber, L. (1981) Towards a unified brain theory. Journal Social Biological Structures. 4, 211-224. [URL http://www.ingber.com/smni81_unified.pdf]

Ingber, L. (1982) Statistical mechanics of neocortical interactions. I. Basic formulation. Physica D. 5, 83-107. [URL http://www.ingber.com/smni82_basic.pdf]

Ingber, L. (1983) Statistical mechanics of neocortical interactions. Dynamics of synaptic modification. Physical Review A. 28, 395-416. [URL http://www.ingber.com/smni83_dynamics.pdf]

Ingber, L. (1984) Statistical mechanics of neocortical interactions. Derivation of short-term-memory capacity. Physical Review A. 29, 3346-3358. [URL http://www.ingber.com/smni84_stm.pdf]

Ingber, L. (1985a) Statistical mechanics algorithm for response to targets (SMART), In: Workshop on Uncertainty and Probability in Artificial Intelligence: UC Los Angeles, 14-16 August 1985, American Association for Artificial Intelligence, 258-264. [URL http://www.ingber.com/combat85_smart.pdf]

Ingber, L. (1985b) Statistical mechanics of neocortical interactions. EEG dispersion relations. IEEE Transactions Biomedical Engineering. 32, 91-94. [URL http://www.ingber.com/smni85_eeg.pdf]

Ingber, L. (1985c) Statistical mechanics of neocortical interactions: Stability and duration of the 7+-2 rule of short-term-memory capacity. Physical Review A. 31, 1183-1186. [URL http://www.ingber.com/smni85_stm.pdf]

Ingber, L. (1986) Statistical mechanics of neocortical interactions. Bulletin American Physical Society. 31, 868.

Ingber, L. (1991) Statistical mechanics of neocortical interactions: A scaling paradigm applied to electroencephalography. Physical Review A. 44(6), 4017-4060. [URL http://www.ingber.com/smni91_eeg.pdf]

Ingber, L. (1992) Generic mesoscopic neural networks based on statistical mechanics of neocortical interactions. Physical Review A. 45(4), R2183-R2186. [URL http://www.ingber.com/smni92_mnn.pdf]

Ingber, L. (1993) Adaptive Simulated Annealing (ASA). Global optimization C-code. Caltech Alumni Association. [URL http://www.ingber.com/#ASA-CODE]

Ingber, L. (1994) Statistical mechanics of neocortical interactions: Path-integral evolution of short-term memory. Physical Review E. 49(5B), 4652-4664. [URL http://www.ingber.com/smni94_stm.pdf]

Ingber, L. (1995a) Statistical mechanics of multiple scales of neocortical interactions, In: Neocortical Dynamics and Human EEG Rhythms, ed. P.L. Nunez. Oxford University Press, 628-681. [ISBN 0-19-505728-7. URL http://www.ingber.com/smni95_scales.pdf]

Ingber, L. (1995b) Statistical mechanics of neocortical interactions: Constraints on 40 Hz models of short-term memory. Physical Review E. 52(4), 4561-4563. [URL http://www.ingber.com/smni95_stm40hz.pdf]

Ingber, L. (1996a) Nonlinear nonequilibrium nonquantum nonchaotic statistical mechanics of neocortical interactions. Behavioral and Brain Sciences. 19(2), 300-301. [Invited commentary on Dynamics

of the brain at global and microscopic scales: Neural networks and the EEG, by J.J. Wright and D.T.J. Liley. URL http://www.ingber.com/smni96_nonlinear.pdf]

Ingber, L. (1996b) Statistical mechanics of neocortical interactions: Multiple scales of EEG, In: Frontier Science in EEG: Continuous Waveform Analysis (Electroencephalography Clinical Neurophysiology Suppl. 45), ed. R.M. Dasheiff & D.J. Vincent. Elsevier, 79-112. [Invited talk to Frontier Science in EEG Symposium, New Orleans, 9 Oct 1993. ISBN 0-444-82429-4. URL http://www.ingber.com/smni96_eeg.pdf]

Ingber, L. (1997) Statistical mechanics of neocortical interactions: Applications of canonical momenta indicators to electroencephalography. Physical Review E. 55(4), 4578-4593. [URL http://www.ingber.com/smni97_cmi.pdf]

Ingber, L. (1998) Statistical mechanics of neocortical interactions: Training and testing canonical momenta indicators of EEG. Mathematical Computer Modelling. 27(3), 33-64. [URL http://www.ingber.com/smni98_cmi_test.pdf]

Ingber, L. (1999) Statistical mechanics of neocortical interactions: Reaction time correlates of the g factor. Psycholoquy. 10(068). [Invited commentary on The g Factor: The Science of Mental Ability by Arthur Jensen. URL http://www.ingber.com/smni99_g_factor.pdf]

Ingber, L. (2000) High-resolution path-integral development of financial options. Physica A. 283(3-4), 529-558. [URL http://www.ingber.com/markets00_highres.pdf]

Ingber, L. (2005) Trading in Risk Dimensions (TRD). Report 2005:TRD. Lester Ingber Research. [URL http://www.ingber.com/markets05_trd.pdf]

Ingber, L. (2006) Ideas by statistical mechanics (ISM). Report 2006:ISM. Lester Ingber Research. [URL http://www.ingber.com/smni06_ism.pdf]

Ingber, L. (2007) Ideas by Statistical Mechanics (ISM). Journal Integrated Systems Design and Process Science. 11(3), 31-54. [Special Issue: Biologically Inspired Computing.]

Ingber, L. (2008) AI and Ideas by Statistical Mechanics (ISM), In: Encyclopedia of Artificial Intelligence, ed. J.R. Rabuñal, J. Dorado & A.P. Pazos. Information Science Reference, 58-64. [ISBN 978-1-59904-849-9]

Ingber, L. (2009a) Statistical mechanics of neocortical interactions: Columnar EEG. Report 2009:CEEG. Lester Ingber Research. [URL http://www.ingber.com/smni09_columnar_eeg.pdf]

Ingber, L. (2009b) Statistical mechanics of neocortical interactions: Nonlinear columnar electroencephalography. NeuroQuantology Journal. 7(4), 500-529. [URL http://www.ingber.com/smni09_nonlin_column_eeg.pdf]

Ingber, L. (2010) Trading in Risk Dimensions, In: The Handbook of Trading: Strategies for Navigating and Profiting from Currency, Bond, and Stock Markets, ed. G.N. Gregoriou. McGraw-Hill, 287-300.

Ingber, L. (2011) Computational algorithms derived from multiple scales of neocortical processing, In: Pointing at Boundaries: Integrating Computation and Cognition on Biological Grounds, ed. A. Pereira, Jr., E. Massad & N. Bobbitt. Springer, 1-13. [Invited Paper. doi: 10.1007/s12559-011-9105-4]

Ingber, L. (2012) Adaptive Simulated Annealing, In: Stochastic global optimization and its applications with fuzzy adaptive simulated annealing, ed. H.A. Oliveira, Jr., A. Petraglia, L. Ingber, M.A.S. Machado & M.R. Petraglia. Springer, 33-61. [Invited Paper. URL http://www.ingber.com/asa11_options.pdf]

Ingber, L., Chen, C., Mondescu, R.P., Muzzall, D. & Renedo, M. (2001) Probability tree algorithm for general diffusion processes. Physical Review E. 64(5), 056702-056707. [URL http://www.ingber.com/path01_pathtree.pdf]

Ingber, L., Fujio, H. & Wehner, M.F. (1991) Mathematical comparison of combat computer models to exercise data. Mathematical Computer Modelling. 15(1), 65-90. [URL http://www.ingber.com/combat91_data.pdf]

Ingber, L. & Nunez, P.L. (1990) Multiple scales of statistical physics of neocortex: Application to electroencephalography. Mathematical Computer Modelling. 13(7), 83-95.

Ingber, L. & Nunez, P.L. (1995) Statistical mechanics of neocortical interactions: High resolution path-integral calculation of short-term memory. Physical Review E. 51(5), 5074-5083. [URL http://www.ingber.com/smni95_stm.pdf]

Ingber, L. & Nunez, P.L. (2010) Neocortical Dynamics at Multiple Scales: EEG Standing Waves, Statistical Mechanics, and Physical Analogs. Mathematical Biosciences. 229, 160-173. [doi:10.1016/j.mbs.2010.12.003 URL http://www.ingber.com/smni10_multiple_scales.pdf]

Irimia, A., Swinney, K.R. & Wikswo, J.P. (2009) Partial independence of bioelectric and biomagnetic field and its implications for encephalography and cardiography. Physical Review E. 79(051908), 1-13.

Jackson, J.D. (1962) Classical Electrodynamics. Wiley & Sons, New York.

Jensen, A. (1987) Individual differences in the Hick paradigm, In: Speed of Information-Processing and Intelligence, ed. P.A. Vernon. Ablex, 101-175.

Jirsa, V.K. & Haken, H. (1996) Field theory of electromagnetic brain activity. Physical Review Letters. 77(5), 960-963.

Johnsen, S. & Lohmann, K.L. (2008) Magnetoreception in animals. Physics Today. 61, 29-35.

Katz, B. (1966) Nerve, Muscle, and Synapse. McGraw-Hill, new York, NY.

Kominis, I.K. (2009) Zeno is pro Darwin: quantum Zeno effect suppresses the dependence of radical-ion-pair reaction yields on exchange and dipolar interactions. arXiv:0908.0763v2 [quant-ph]. University of Crete.

Korn, H. & Mallet, A. (1984) Transformation of binomial input by the postsynaptic membrane at a central synapse. Science. 225, 1157-1159.

Korn, H., Mallet, A. & Faber, D.S. (1981) Fluctuating responses at a central synapse: *n* of binomial fit predicts number of stained presynaptic boutons. Science. 213, 898-900.

Langouche, F., Roekaerts, D. & Tirapegui, E. (1979) Discretization problems of functional integrals in phase space. Physical Review D. 20, 419-432.

Langouche, F., Roekaerts, D. & Tirapegui, E. (1982) Functional Integration and Semiclassical Expansions. Reidel, Dordrecht, The Netherlands.

Little, W.A. (1974) The existence of persistent states in the brain. Mathematical Biosciences. 19, 101-120.

Little, W.A. & Shaw, G.L. (1978) Analytic study of the memory storage capacity of a neural network. Mathematical Biosciences. 39, 281-290.

Markram, H., Toledo-Rodriguez, M., Wang, Y., Gupta, A., Silberberg, G. & Wu, C. (2004) Interneurons of the neocortical inhibitory system. Nature Reviews. 5, 793-807.

Mathews, J. & Walker, R.L. (1970) Mathematical Methods of Physics, 2nd ed.. Benjamin, New York, NY.

McFadden, J. (2007) Conscious electromagnetic field theory. NeuroQuantology. 5(3), 262-270.

Miller, G.A. (1956) The magical number seven, plus or minus two. Psychology Review. 63, 81-97.

Moore, C.I. & Cao, R. (2008) The hemo-neural hypothesis: On the role of blood flow in information processing. Journal of Neurophysiology. 99, 2035-2047.

Mountcastle, V.B. (1978) An organizing principle for cerebral function: The unit module and the distributed system, In: The Mindful Brain, ed. G.M. Edelman & V.B. Mountcastle. Massachusetts Institute of Technology, 7-50.

Mountcastle, V.B., Andersen, R.A. & Motter, B.C. (1981) The influence of attentive fixation upon the excitability of the light-sensitive neurons of the posterior parietal cortex. Journal of Neuroscience. 1, 1218-1235.

Murakami, S. & Okada, Y. (2006) Contributions of principal neocortical neurons to magnetoencephalography and electroencephalography signals. Journal of Physiology. 575(3), 925-936.

Murdock, B.B., Jr. (1983) A distributed memory model for serial-order information. Psychology Review. 90, 316-338.

Nakano, T., Suda, T., Koujin, T., Haraguchi, T. & Hiraoka, Y. (2007) Molecular communication through gap junction channels: System design, experiments and modeling, In: Proceedings 2nd International Conference on Bio-Inspirred Models of Network, Information, and Computing Systems, Institute for Computer Sciences, Social-Informatics and Telecommunications Engineering, 139-146.

Nunez, P.L. (1981) Electric Fields of the Brain: The Neurophysics of EEG. Oxford University Press, London.

Nunez, P.L. (1989) Generation of human EEG rhythms by a combination of long and short-range neocortical interactions. Brain Topography. 1, 199-215.

Nunez, P.L. & Srinivasan, R. (2006) Electric Fields of the Brain: The Neurophysics of EEG, 2nd Ed.. Oxford University Press, London.

Oberheim, N.A., Takano, T., Han, X., He, W., Lin, J.H.C., Wang, F., Xu, Q., Wyatt, J.D., Pilcher, W., Ojemann, J.G., Ransom, B.R., Goldman, S.A. & Nedergaard, M. (2009) Uniquely hominid features of adult human astrocytes. Journal of Neuroscience. 29(10), 3276-3287.

Pereira, A., Jr. & Furlan, F.A. (2009) On the role of synchrony for neuron-astrocyte interactions and perceptual conscious processing. Journal of Biological Physics. 35(4), 465-480.

Pereira, A., Jr. & Furlan, F.A. (2010) Astrocytes and human cognition: Modeling information integration and modulation of neuronal activity. Progress in Neurobiology. 92, 405-420.

Perkel, D.H. & Feldman, M.W. (1979) Neurotransmitter release statistics: Moment estimates for inhomogeneous Bernoulli trials. Journal of Mathematical Biology. 7, 31-40.

Postnov, D.E., Koreshkov, R.N., Brazhe, N.A., Brazhe, A.R. & Sosnovtseva, O.V. (2009) Dynamical patterns of calcium signaling in a functional model of neuron-astrocyte networks. Journal of Biological Physics. 35, 425-445.

Rabinovich, M.I., Varona, P., Selverston, A.I. & Arbaranel, H.D.I. (2006) Dynamical principles in neuroscience. Reviews Modern Physics. 78(4), 1213-1265.

Rakic, P. (2008) Confusing cortical columns. Proceedings of the National Academy of Sciences. 105(34), 12099-12100. [URL http://www.pnas.org/content/105/34/12099.full]

Reisin, H.D. & Colombo, J.A. (2002) Considerations on the astroglial architecture and the columnar organization of the cerebral cortex. Cellular and Molecular Neurobiology. 22(5/6), 633-644.

Risken, H. (1989) The Fokker-Planck Equation: Methods of Solution and Applications. Springer-Verlag, Berlin.

Rodgers, C.T. & Hore, P.J. (2009) Chemical magnetoreception in birds: The radical pair mechanism. Proceedings of the National Academy of Sciences. 106(2), 353-360.

Roth, B.J. & Wikswo, J.P., Jr. (1985) The magnetic field of a single axon. Biophysical Journal. 48, 93-109.

Scemes, E., Suadicani, S.O. & Spray, D.C. (2000) Intercellular calcium wave communication via gap junction dependent and independent mechanisms, In: Current Topics in Membranes, Academic Press, 145-173.

Schipke, C.G., Boucsein, C., Ohlemeyer, C., Kirchhoff, F. & Kettenmann, H. (2002) Astrocyte Ca2+ waves trigger responses in microglial cells in brain slices. Federation of American Societies for Experimental Biology Journal. 16, 255-257.

Schulman, L.S. (1981) Techniques and Applications of Path Integration. J. Wiley & Sons, New York.

Scott, A.C. (1975) The electrophysics of a nerve fiber. Reviews Modern Physics. 47, 487-533.

Shaw, G.L. & Vasudevan, R. (1974) Persistent states of neural networks and the random nature of synaptic transmission. Mathematical Biosciences. 21, 207-218.

Shepherd, G.M. (1979) The Synaptic Organization of the Brain, 2nd ed.. Oxford University Press, New York, NY.

Silberstein, R.N. (1995) Neuromodulation of neocortical dynamics, In: Neocortical Dynamics and Human EEG Rhythms, ed. P.L. Nunez. Oxford University Press, 628-681.

Solov'yov, I.A. & Schulten, K. (2009) Magnetoreception through cryptochrome may involve superoxide. Biophysical Journal. 96(12), 4804-4813.

Sommerhoff, G. (1974) Logic of the Living Brain. Wiley, New York, NY.

Tollaksen, J., Aharonov, Y., Casher, A., Kaufherr, T. & Nussinov, S. (2010) Quantum interference experiments, modular variables and weak measurements. New Journal of Physics. 12(013023), 1-29.

Tsal, Y. (1983) Movements of attention across the visual field. Journal of Experimental Psychology. 9, 523-530.

von der Heydt, I., von der Heydt, N. & Obermair, G.M. (1981) Statistical model of current-coupled ion channels in nerve membranes. Zeitschrift für Physik. 41, 153-164.

Vu, E.T. & Krasne, F.B. (1992) Evidence for a computational distinction between proximal and distal neuronal inhibition. Science. 255, 1710-1712.

Zhang, G. & Simon, H.A. (1985) STM capacity for Chinese words and idioms: Chunking and acoustical loop hypotheses. Memory & Cognition. 13, 193-201.

Zhang, X.L., Begleiter, H., Porjesz, B., Wang, W. & Litke, A. (1995) Event related potentials during object recognition tasks. Brain Research Bulletin. 38(6), 531-538.